Immersion freezing in particle-based cloud microphysics models

S. Arabas[1,2], J.H. Curtis[1], I. Silber[3], A. Fridlind[4], D.A Knopf[5], M. West[1] & N. Riemer[1]

1: atmos.illinois.edu
2: uj.edu.pl
3: met.psu.edu
4: giss.nasa.gov
5: stonybrook.edu

funding: ASR Atmospheric System Research

2nd QuIESCENT Workshop, Arctic Science Summit Week, Tromsø (virtual), Apr 1 2022

super-particles as a probabilistic alternative to bulk or bin μ-physics

JAMES | Journal of Advances in Modeling Earth Systems

COMMISSIONED MANUSCRIPT
10.1029/2019MS001689

Key Points:
- Microphysics is an important component of weather and climate models, but its representation in current models is highly uncertain

Confronting the Challenge of Modeling Cloud and Precipitation Microphysics

Hugh Morrison[1], Marcus van Lier-Walqui[2], Ann M. Fridlind[3], Wojciech W. Grabowski[1], Jerry Y. Harrington[4], Corinna Hoose[5], Alexei Korolev[6], Matthew R. Kumjian[4], Jason A. Milbrandt[7], Hanna Pawlowska[8], Derek J. Posselt[9], Olivier P. Prat[10], Karly J. Reimel[4], Shin-Ichiro Shima[11], Bastiaan van Diedenhoven[2], and Lulin Xue[1]

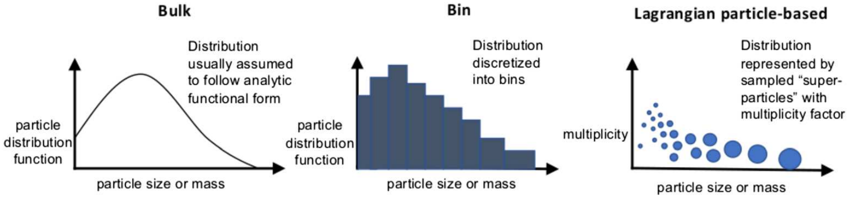

Figure 3. Representation of cloud and precipitation particle distributions in the three main types of microphysics

super-particles as a probabilistic alternative to bulk or bin μ-physics

JAMES | Journal of Advances in Modeling Earth Systems

COMMISSIONED MANUSCRIPT
10.1029/2019MS001689

Confronting the Challenge of Modeling Cloud and Precipitation Microphysics

Hugh Morrison[1], Marcus van Lier-Walqui[2], Ann M. Fridlind[3], Wojciech W. Grabowski[1], Jerry Y. Harrington[4], Corinna Hoose[5], Alexei Korolev[6], Matthew R. Kumjian[4], Jason A. Milbrandt[7], Hanna Pawlowska[8], Derek J. Posselt[9], Olivier P. Prat[10], Karly J. Reimel[4], Shin-Ichiro Shima[11], Bastiaan van Diedenhoven[2], and Lulin Xue[1]

Key Points:
- Microphysics is an important component of weather and climate models, but its representation in current models is highly uncertain

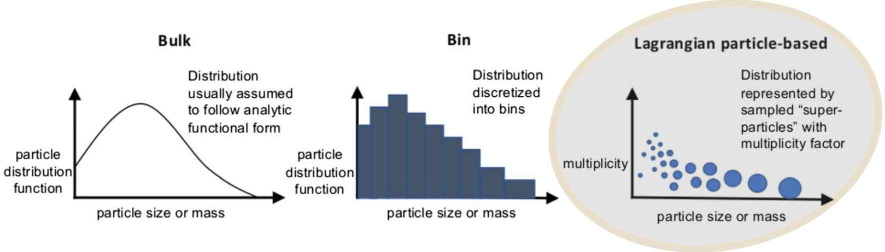

Figure 3. Representation of cloud and precipitation particle distributions in the three main types of microphysics

Shima et al. '20 particle-based mixed-phase μ-physics

Shima, Sato, Hashimoto & Misumi 2020 (GMD):
Predicting the morphology of ice particles in deep convection using the super-droplet method

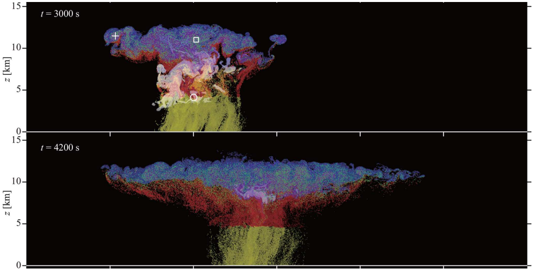

Figure 1. Typical realization of CTRL cloud spatial structures at $t = 2040$, 2460, 3000, 4200, and 5400 s. The mixing ratio of cloud water, rainwater, cloud ice, graupel, and snow aggregates are plotted in fading white, yellow, blue, red, and green, respectively. The symbols indicate examples of unrealistic predicted ice particles (Sects. 7.3 and 9.1). See also Movie 1 in the video supplement.

Shima et al. ’20 particle-based mixed-phase μ-physics

Shima, Sato, Hashimoto & Misumi 2020 (GMD):

Predicting the morphology of ice particles in deep convection using the super-droplet method

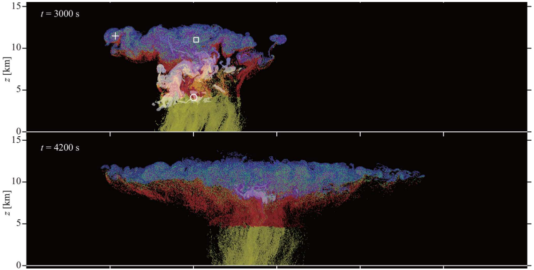

Figure 1. Typical realization of CTRL cloud spatial structures at $t = 2040$, 2460, 3000, 4200, and 5400 s. The mixing ratio of cloud water, rainwater, cloud ice, graupel, and snow aggregates are plotted in fading white, yellow, blue, red, and green, respectively. The symbols indicate examples of unrealistic predicted ice particles (Sects. 7.3 and 9.1). See also Movie 1 in the video supplement.

- Eulerian component: momentum, heat, moisture budget

Shima, Sato, Hashimoto & Misumi 2020 (GMD):

Predicting the morphology of ice particles in deep convection using the super-droplet method

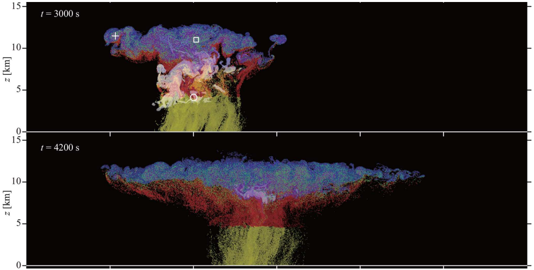

Figure 1. Typical realization of CTRL cloud spatial structures at $t = 2040$, 2460, 3000, 4200, and 5400 s. The mixing ratio of cloud water, rainwater, cloud ice, graupel, and snow aggregates are plotted in fading white, yellow, blue, red, and green, respectively. The symbols indicate examples of unrealistic predicted ice particles (Sects. 7.3 and 9.1). See also Movie 1 in the video supplement.

- Eulerian component: momentum, heat, moisture budget
- Lagrangian component: super particles representing aerosol, water droplets, ice particles (porous spheroids)

Shima et al. '20 particle-based mixed-phase μ-physics

Shima, Sato, Hashimoto & Misumi 2020 (GMD):

Predicting the morphology of ice particles in deep convection using the super-droplet method

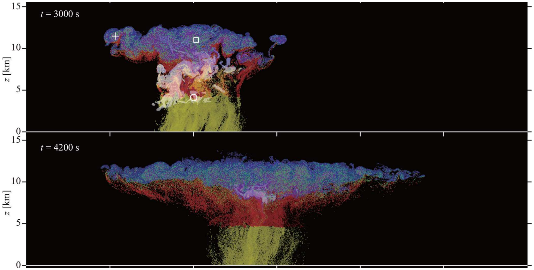

Figure 1. Typical realization of CTRL cloud spatial structures at $t = 2040$, 2460, 3000, 4200, and 5400 s. The mixing ratio of cloud water, rainwater, cloud ice, graupel, and snow aggregates are plotted in fading white, yellow, blue, red, and green, respectively. The symbols indicate examples of unrealistic predicted ice particles (Sects. 7.3 and 9.1). See also Movie 1 in the video supplement.

- Eulerian component: momentum, heat, moisture budget
- Lagrangian component: super particles representing aerosol, water droplets, ice particles (porous spheroids)
- particle-resolved processes:
  — advection and sedimentation
  — homogeneous and immersion freezing (singular)
  — melting
  — condensation and evaporation (incl. CCN [de]activation)
  — deposition and sublimation
  — collisions (coalescence, riming, aggregation, washout)

Shima, Sato, Hashimoto & Misumi 2020 (GMD):
Predicting the morphology of ice particles in deep convection using the super-droplet method

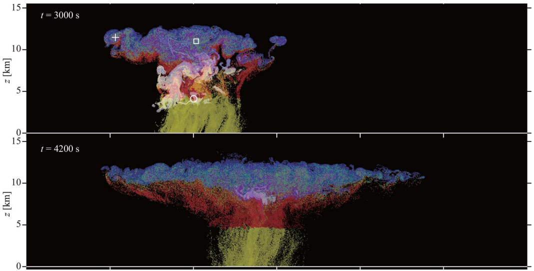

Figure 1. Typical realization of CTRL cloud spatial structures at $t = 2040$, 2460, 3000, 4200, and 5400 s. The mixing ratio of cloud water, rainwater, cloud ice, graupel, and snow aggregates are plotted in fading white, yellow, blue, red, and green, respectively. The symbols indicate examples of unrealistic predicted ice particles (Sects. 7.3 and 9.1). See also Movie 1 in the video supplement.

- Eulerian component: momentum, heat, moisture budget
- Lagrangian component: super particles representing aerosol, water droplets, ice particles (porous spheroids)
- particle-resolved processes:
  — advection and sedimentation
  — homogeneous and immersion freezing (singular)
  — melting
  — condensation and evaporation (incl. CCN [de]activation)
  — deposition and sublimation
  — collisions (coalescence, riming, aggregation, washout)
- 2D Cb test case

Shima et al. '20 particle-based mixed-phase μ-physics

Shima, Sato, Hashimoto & Misumi 2020 (GMD):

Predicting the morphology of ice particles in deep convection using the super-droplet method

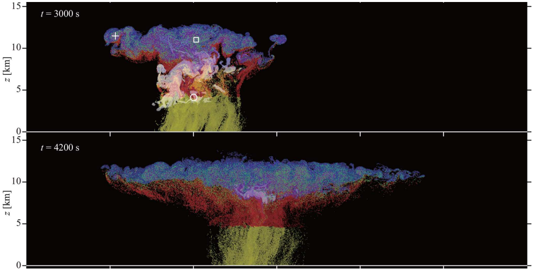

Figure 1. Typical realization of CTRL cloud spatial structures at $t = 2040$, 2460, 3000, 4200, and 5400 s. The mixing ratio of cloud water, rainwater, cloud ice, graupel, and snow aggregates are plotted in fading white, yellow, blue, red, and green, respectively. The symbols indicate examples of unrealistic predicted ice particles (Sects. 7.3 and 9.1). See also Movie 1 in the video supplement.

- Eulerian component: momentum, heat, moisture budget
- Lagrangian component: super particles representing aerosol, water droplets, ice particles (porous spheroids)

- particle-resolved processes:
  — advection and sedimentation
  — homogeneous and immersion freezing (singular)
  — melting
  — condensation and evaporation (incl. CCN [de]activation)
  — deposition and sublimation
  — collisions (coalescence, riming, aggregation, washout)

- 2D Cb test case

Poissonian model of freezing & Ice Nucleation Active Sites (INAS)

theory (in modern notation)
(Bigg '53, Langham & Mason '58, Carte '59, Marshall '61)

Poissonian model of freezing & Ice Nucleation Active Sites (INAS)

theory (in modern notation)
(Bigg '53, Langham & Mason '58, Carte '59, Marshall '61)

Poisson counting process with rate r:

$$P^*(\text{k events in time t}) = \frac{(rt)^k \exp(-rt)}{k!}$$

$$P(\text{one or more events in time t}) = 1 - P^*(k=0, t)$$

$$\ln(1-P) = -rt$$

Poissonian model of freezing & Ice Nucleation Active Sites (INAS)

theory (in modern notation)
(Bigg '53, Langham & Mason '58, Carte '59, Marshall '61)

Poisson counting process with rate r:

$$P^*(\text{k events in time t}) = \frac{(rt)^k \exp(-rt)}{k!}$$

$$P(\text{one or more events in time t}) = 1 - P^*(k=0, t)$$

$$\ln(1-P) = -rt$$

introducing $J_{\text{het}}(T)$, $T(t)$ and INP surface A:

$$\ln\left(1-P(A,t)\right) = -A \underbrace{\int_0^t J_{\text{het}}(T(t'))\,dt'}_{I(T)}$$

Poissonian model of freezing & Ice Nucleation Active Sites (INAS)

theory (in modern notation)
(Bigg '53, Langham & Mason '58, Carte '59, Marshall '61)

Poisson counting process with rate r:

$$P^*(\text{k events in time t}) = \frac{(rt)^k \exp(-rt)}{k!}$$

$$P(\text{one or more events in time t}) = 1 - P^*(k=0, t)$$

$$\ln(1-P) = -rt$$

introducing $J_{\text{het}}(T)$, $T(t)$ and INP surface A:

$$\ln\left(1 - P(A,t)\right) = \underbrace{-A \int_0^t J_{\text{het}}(T(t'))\, dt'}_{I(T)}$$

INAS: $$I(T) = n_s(T) = \exp(a \cdot (T - T_{0^\circ C}) + b)$$

Poissonian model of freezing & Ice Nucleation Active Sites (INAS)

theory (in modern notation)
(Bigg '53, Langham & Mason '58, Carte '59, Marshall '61)

Poisson counting process with rate r:

$$P^*(\text{k events in time t}) = \frac{(rt)^k \exp(-rt)}{k!}$$

$$P(\text{one or more events in time t}) = 1 - P^*(k=0,t)$$

$$\ln(1-P) = -rt$$

introducing $J_{\text{het}}(T)$, $T(t)$ and INP surface A:

$$\ln\left(1 - P(A,t)\right) = -A \underbrace{\int_0^t J_{\text{het}}(T(t'))\,dt'}_{I(T)}$$

INAS: $$I(T) = n_s(T) = \exp(a \cdot (T - T_{0^\circ C}) + b)$$

experimental $n_s(T)$ fits: e.g., Niemand et al. 2012

particle-based freezing: singular (Shima et al.) / time-dependent (this work)

singular: INAS T_{fz} **as attribute**; initialisation by random sampling from $P(T_{fz}, A)$ with lognormal A (A is not an attribute, initialisation only); freezing if $T(t) < T_{fz}(t = 0)$

time-dependent: A **as attribute** (randomly sampled from the same lognormal) Monte-Carlo freezing trigger using $P(J_{het}(T(t)))$

singular (INAS)

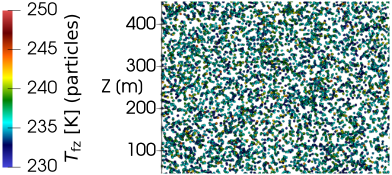

time-dependent (ABIFM)

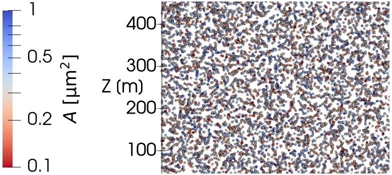

particle-based freezing: singular (Shima et al.) / time-dependent (this work)

singular: INAS T_{fz} **as attribute**; initialisation by random sampling from $P(T_{fz}, A)$ with lognormal A (A is not an attribute, initialisation only); freezing if $T(t) < T_{fz}(t=0)$

time-dependent: A **as attribute** (randomly sampled from the same lognormal)
Monte-Carlo freezing trigger using $P(J_{het}(T(t)))$

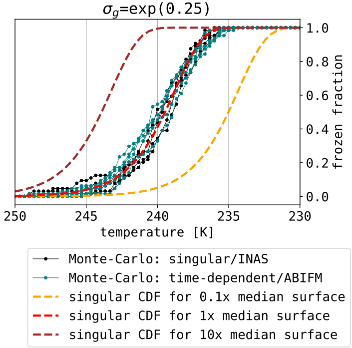

particle-based freezing: singular (Shima et al.) / time-dependent (this work)

singular: INAS T_{fz} **as attribute**; initialisation by random sampling from $P(T_{fz}, A)$ with lognormal A (A is not an attribute, initialisation only); freezing if $T(t) < T_{fz}(t=0)$

time-dependent: A **as attribute** (randomly sampled from the same lognormal) Monte-Carlo freezing trigger using $P(J_{het}(T(t)))$

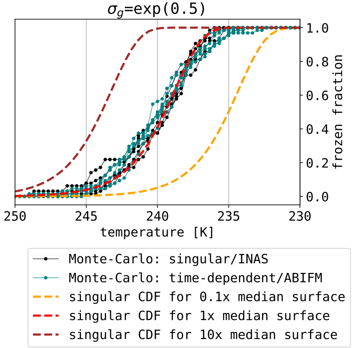

particle-based freezing: singular (Shima et al.) / time-dependent (this work)

singular: INAS T_{fz} **as attribute**; initialisation by random sampling from $P(T_{\text{fz}}, A)$ with lognormal A (A is not an attribute, initialisation only); freezing if $T(t) < T_{fz}(t = 0)$

time-dependent: A **as attribute** (randomly sampled from the same lognormal) Monte-Carlo freezing trigger using $P(J_{\text{het}}(T(t)))$

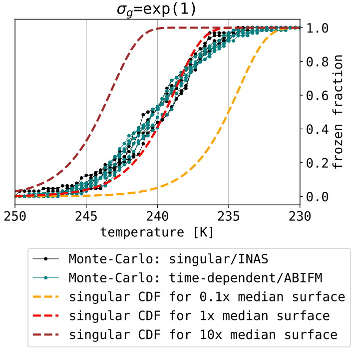

particle-based freezing: singular (Shima et al.) / time-dependent (this work)

singular: INAS T_{fz} **as attribute**; initialisation by random sampling from $P(T_{\rm fz}, A)$ with lognormal A (A is not an attribute, initialisation only); freezing if $T(t) < T_{fz}(t=0)$

time-dependent: A **as attribute** (randomly sampled from the same lognormal)
Monte-Carlo freezing trigger using $P(J_{\rm het}(T(t)))$

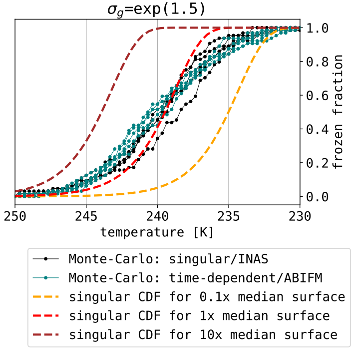

particle-based freezing: singular (Shima et al.) / time-dependent (this work)

singular: INAS T_{fz} **as attribute**; initialisation by random sampling from $P(T_{fz}, A)$ with lognormal A (A is not an attribute, initialisation only); freezing if $T(t) < T_{fz}(t=0)$

time-dependent: A **as attribute** (randomly sampled from the same lognormal) Monte-Carlo freezing trigger using $P(J_{het}(T(t)))$

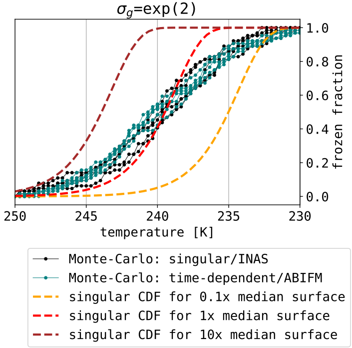

particle-based freezing: singular (Shima et al.) / time-dependent (this work)

singular: INAS T_{fz} **as attribute**; initialisation by random sampling from $P(T_{fz}, A)$ with lognormal A (A is not an attribute, initialisation only); freezing if $T(t) < T_{fz}(t = 0)$

time-dependent: A **as attribute** (randomly sampled from the same lognormal) Monte-Carlo freezing trigger using $P(J_{het}(T(t)))$

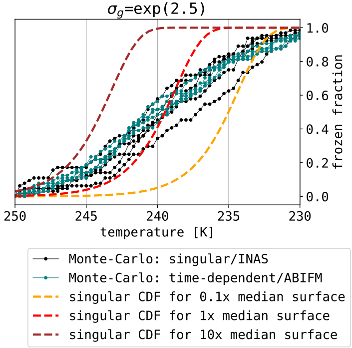

particle-based freezing: singular (Shima et al.) / time-dependent (this work)

singular: INAS T_{fz} **as attribute**; initialisation by random sampling from $P(T_{fz}, A)$ with lognormal A (A is not an attribute, initialisation only); freezing if $T(t) < T_{fz}(t = 0)$

time-dependent: A **as attribute** (randomly sampled from the same lognormal) Monte-Carlo freezing trigger using $P(J_{het}(T(t)))$

AIDA cooling rate: $0.5\ {}^{K}/_{min}$

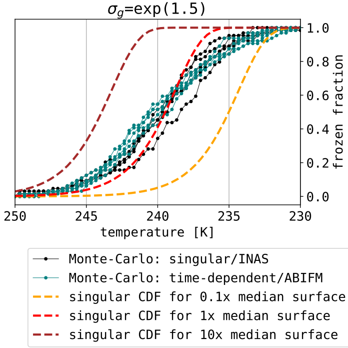

particle-based freezing: singular (Shima et al.) / time-dependent (this work)

singular: INAS T_{fz} **as attribute**; initialisation by random sampling from $P(T_{fz}, A)$ with lognormal A (A is not an attribute, initialisation only); freezing if $T(t) < T_{fz}(t=0)$

time-dependent: A **as attribute** (randomly sampled from the same lognormal) Monte-Carlo freezing trigger using $P(J_{het}(T(t)))$

cooling rate: 0.1 $^K/_{min}$

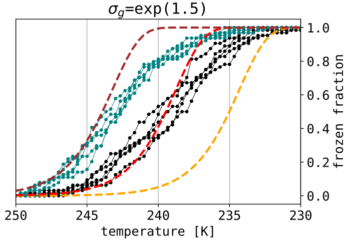

AIDA cooling rate: 0.5 $^K/_{min}$

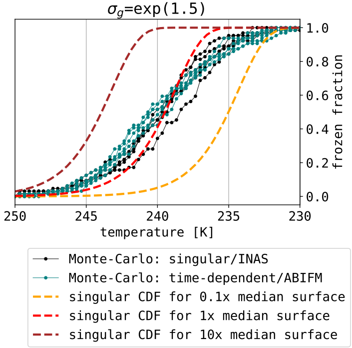

particle-based freezing: singular (Shima et al.) / time-dependent (this work)

singular: INAS T_{fz} **as attribute**; initialisation by random sampling from $P(T_{fz}, A)$ with lognormal A (A is not an attribute, initialisation only); freezing if $T(t) < T_{fz}(t=0)$

time-dependent: A **as attribute** (randomly sampled from the same lognormal) Monte-Carlo freezing trigger using $P(J_{het}(T(t)))$

cooling rate: 0.1 $^{K}/_{min}$

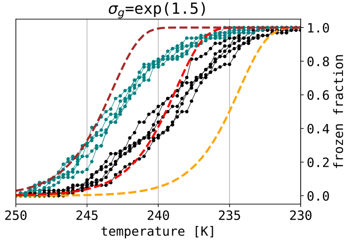

AIDA cooling rate: 0.5 $^{K}/_{min}$

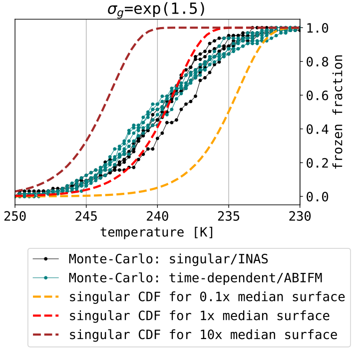

cooling rate: 2.5 $^{K}/_{min}$

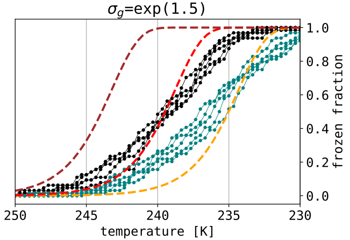

Poissonian model of freezing & Ice Nucleation Active Sites (INAS)

theory (in modern notation)
(Bigg '53, Langham & Mason '58, Carte '59, Marshall '61)

Poisson counting process with rate r:

$$P^*(\text{k events in time t}) = \frac{(rt)^k \exp(-rt)}{k!}$$

$$P(\text{one or more events in time t}) = 1 - P^*(k=0,t)$$

$$\ln(1-P) = -rt$$

introducing $J_{\text{het}}(T)$, $T(t)$ and INP surface A:

$$\ln\left(1-P(A,t)\right) = -A \underbrace{\int_0^t J_{\text{het}}(T(t'))\,dt'}_{I(T)}$$

INAS: $I(T) = n_s(T) = \exp(a \cdot (T - T_{0°C}) + b)$

experimental $n_s(T)$ fits: e.g., Niemand et al. 2012

Poissonian model of freezing & Ice Nucleation Active Sites (INAS)

theory (in modern notation)
(Bigg '53, Langham & Mason '58, Carte '59, Marshall '61)

Poisson counting process with rate r:

$$P^*(\text{k events in time t}) = \frac{(rt)^k \exp(-rt)}{k!}$$

$$P(\text{one or more events in time t}) = 1 - P^*(k=0, t)$$

$$\ln(1-P) = -rt$$

introducing $J_{\text{het}}(T)$, $T(t)$ and INP surface A:

$$\ln\left(1 - P(A,t)\right) = -A \underbrace{\int_0^t J_{\text{het}}(T(t'))\, dt'}_{I(T)}$$

INAS: $I(T) = n_s(T) = \exp(a \cdot (T - T_{0^\circ C}) + b)$

experimental $n_s(T)$ fits: e.g., Niemand et al. 2012

for a constant cooling rate $c = dT/dt$:

$$\ln(1 - P(A,t)) = -\frac{A}{c}\int_{T_0}^{T_0+ct} J_{\text{het}}(T')dT' = -A \cdot I(T)$$

Poissonian model of freezing & Ice Nucleation Active Sites (INAS)

theory (in modern notation)
(Bigg '53, Langham & Mason '58, Carte '59, Marshall '61)

Poisson counting process with rate r:

$$P^*(\text{k events in time t}) = \frac{(rt)^k \exp(-rt)}{k!}$$

$$P(\text{one or more events in time t}) = 1 - P^*(k=0, t)$$

$$\ln(1-P) = -rt$$

introducing $J_{\text{het}}(T)$, $T(t)$ and INP surface A:

$$\ln\left(1 - P(A,t)\right) = -A \underbrace{\int_0^t J_{\text{het}}(T(t'))\, dt'}_{I(T)}$$

INAS: $I(T) = n_s(T) = \exp(a \cdot (T - T_{0^\circ C}) + b)$

experimental $n_s(T)$ fits: e.g., Niemand et al. 2012

for a constant cooling rate $c = dT/dt$:

$$\ln(1 - P(A,t)) = -\frac{A}{c}\int_{T_0}^{T_0+ct} J_{\text{het}}(T')dT' = -A \cdot I(T)$$

$$\frac{dn_s(T)}{dT} = a \cdot n_s(T) = -\frac{1}{c} J_{\text{het}}(T)$$

Poissonian model of freezing & Ice Nucleation Active Sites (INAS)

theory (in modern notation)
(Bigg '53, Langham & Mason '58, Carte '59, Marshall '61)

Poisson counting process with rate r:

$$P^*(\text{k events in time t}) = \frac{(rt)^k \exp(-rt)}{k!}$$

$$P(\text{one or more events in time t}) = 1 - P^*(k=0, t)$$

$$\ln(1-P) = -rt$$

introducing $J_{\text{het}}(T)$, $T(t)$ and INP surface A:

$$\ln\left(1-P(A,t)\right) = \underbrace{-A\int_0^t J_{\text{het}}(T(t'))\,dt'}_{I(T)}$$

INAS: $I(T) = n_s(T) = \exp(a\cdot(T - T_{0^\circ C}) + b)$

experimental $n_s(T)$ fits: e.g., Niemand et al. 2012

for a constant cooling rate $c = dT/dt$:

$$\ln(1-P(A,t)) = -\frac{A}{c}\int_{T_0}^{T_0+ct} J_{\text{het}}(T')dT' = -A\cdot I(T)$$

$$\frac{dn_s(T)}{dT} = a\cdot n_s(T) = -\frac{1}{c}J_{\text{het}}(T)$$

experimental fits: INAS n_s (Niemand et al. '12)
ABIFM J_{het} (Knopf & Alpert '13)

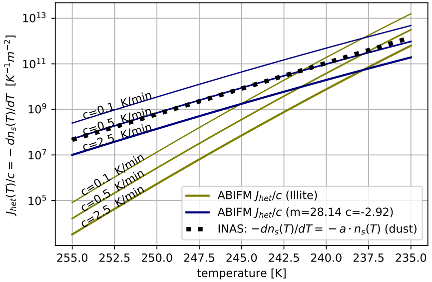

Poissonian model of freezing & Ice Nucleation Active Sites (INAS)

theory (in modern notation)
(Bigg '53, Langham & Mason '58, Carte '59, Marshall '61)

Poisson counting process with rate r:

$$P^*(\text{k events in time t}) = \frac{(rt)^k \exp(-rt)}{k!}$$

$$P(\text{one or more events in time t}) = 1 - P^*(k=0,t)$$

$$\ln(1-P) = -rt$$

introducing $J_{\text{het}}(T)$, $T(t)$ and INP surface A:

$$\ln\left(1-P(A,t)\right) = \underbrace{-A\int_0^t J_{\text{het}}(T(t'))\,dt'}_{I(T)}$$

INAS: $I(T) = n_s(T) = \exp(a \cdot (T - T_{0^\circ C}) + b)$

experimental $n_s(T)$ fits: e.g., Niemand et al. 2012

for a constant cooling rate $c = dT/dt$:

$$\ln(1-P(A,t)) = -\frac{A}{c}\int_{T_0}^{T_0+ct} J_{\text{het}}(T')dT' = -A \cdot I(T)$$

$$\frac{dn_s(T)}{dT} = a \cdot n_s(T) = -\frac{1}{c} J_{\text{het}}(T)$$

experimental fits: INAS n_s (Niemand et al. '12)
ABIFM J_{het} (Knopf & Alpert '13)

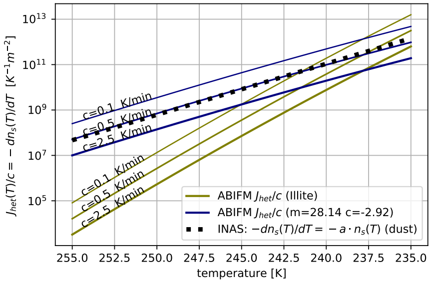

cf. Vali & Stansbury '66; modified singular model (Vali '94, Murray et al. '11)
but the singular ansatz limitation of sampling T_{fz} at t=0 remains

Poissonian model of freezing & Ice Nucleation Active Sites (INAS)

Is it a problem?

for a constant cooling rate $c = dT/dt$:

$$\ln(1 - P(A,t)) = -\frac{A}{c}\int_{T_0}^{T_0+ct} J_{\text{het}}(T')dT' = -A \cdot I(T)$$

$$\frac{dn_s(T)}{dT} = a \cdot n_s(T) = -\frac{1}{c}J_{\text{het}}(T)$$

experimental fits: INAS n_s (Niemand et al. '12)
ABIFM J_{het} (Knopf & Alpert '13)

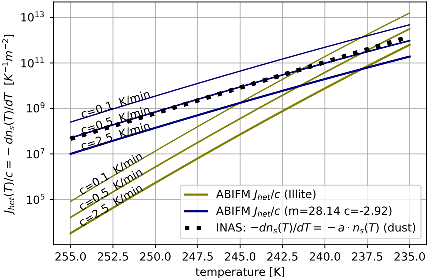

cf. Vali & Stansbury '66; modified singular model (Vali '94, Murray et al. '11)
but the singular ansatz limitation of sampling T_{fz} at t=0 remains

particle-based μ-physics + prescribed-flow test (aka KiD-2D)[a,b,c,d,e]

Lagrangian component (PySDM)

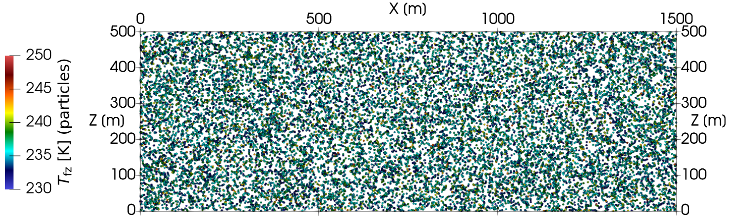

Eulerian component (PyMPDATA)

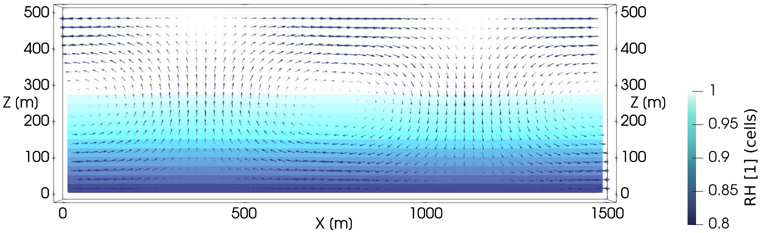

[a] concept: Gedzelman & Arnold '93

[b] stratiform: Morrison & Grabowski '07

[c] particle-based: Arabas et al. '15

[d] KiD-2D: github.com/BShipway/KiD

[e] here: SHEBA case (Fridlind et al. '12)

particle-based μ-physics + prescribed-flow test

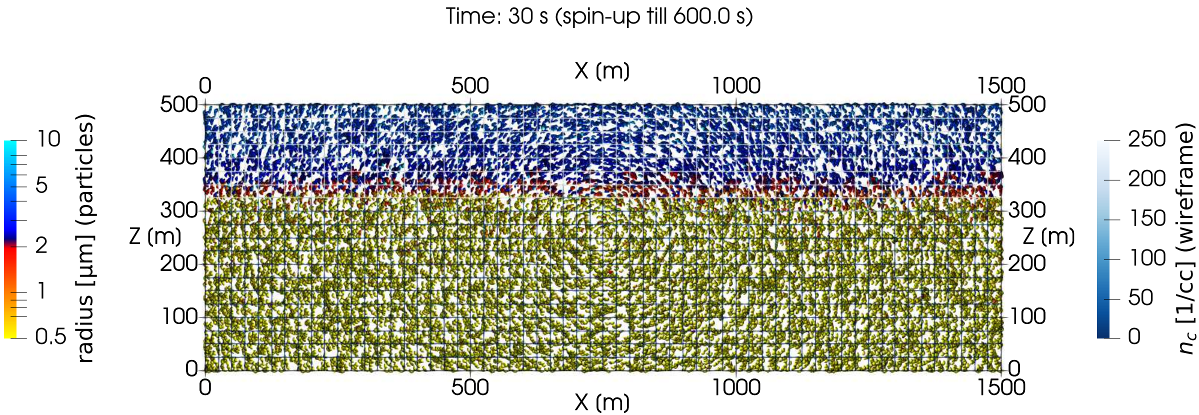

16+16 super-particles/cell for INP-rich + INP-free particles

$N_{aer} = 300/cc$ (two-mode lognormal) $N_{INP} = 150/L$ (lognormal, $D_g = 0.74$ μm, $\sigma_g = 2.55$)

spin-up = freezing off; subsequently frozen particles act as tracers

particle-based μ-physics + prescribed-flow test

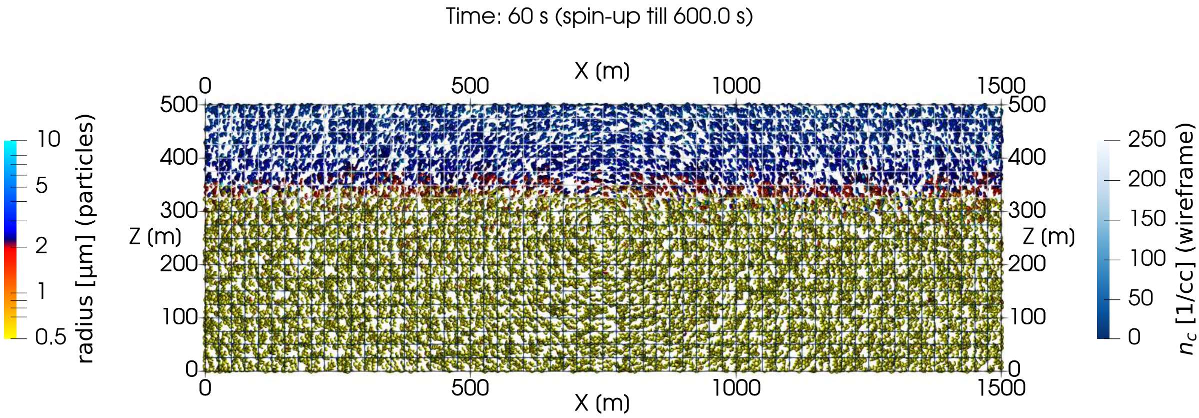

16+16 super-particles/cell for INP-rich + INP-free particles

$N_{\text{aer}} = 300/cc$ (two-mode lognormal) $N_{\text{INP}} = 150/L$ (lognormal, $D_g = 0.74$ μm, $\sigma_g = 2.55$)

spin-up = freezing off; subsequently frozen particles act as tracers

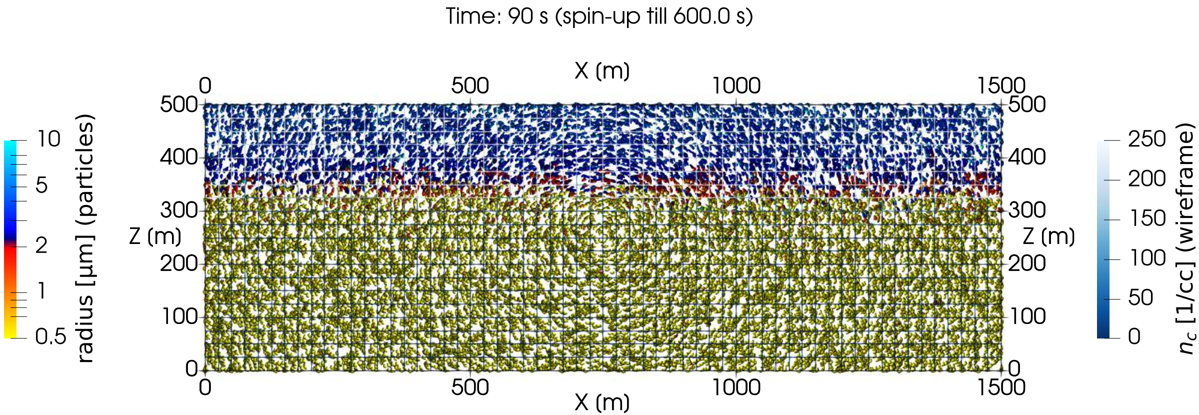

16+16 super-particles/cell for INP-rich + INP-free particles

$N_{aer} = 300/cc$ (two-mode lognormal) $N_{INP} = 150/L$ (lognormal, $D_g = 0.74$ μm, $\sigma_g = 2.55$)

spin-up = freezing off; subsequently frozen particles act as tracers

particle-based μ-physics + prescribed-flow test

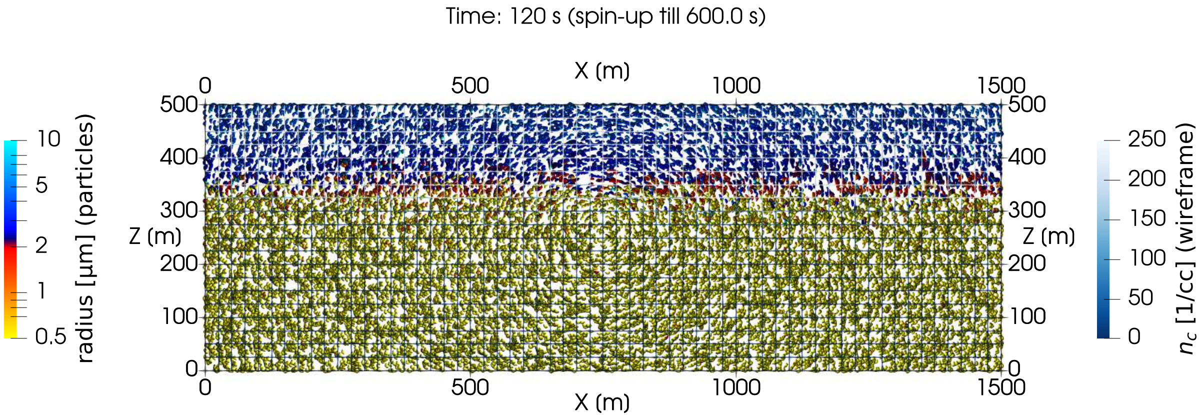

16+16 super-particles/cell for INP-rich + INP-free particles

$N_{aer} = 300/cc$ (two-mode lognormal) $N_{INP} = 150/L$ (lognormal, $D_g = 0.74$ μm, $\sigma_g = 2.55$)

spin-up = freezing off; subsequently frozen particles act as tracers

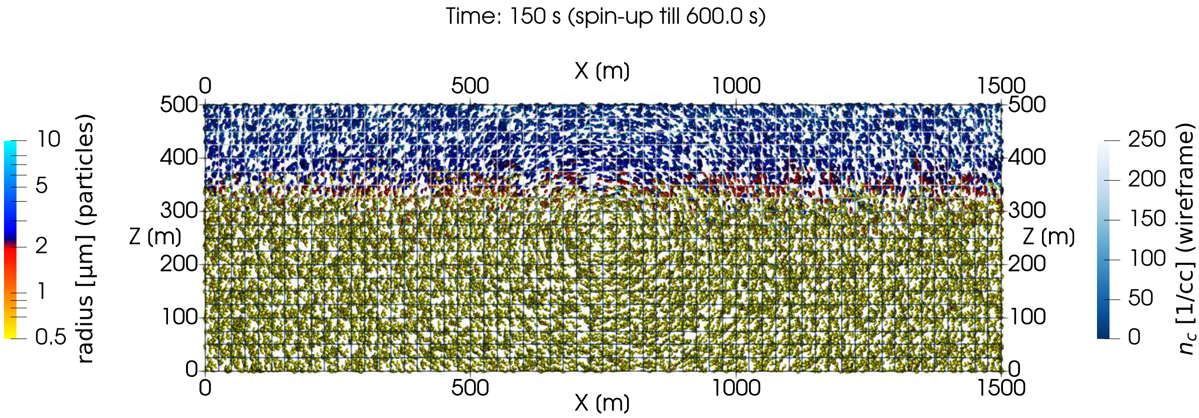

16+16 super-particles/cell for INP-rich + INP-free particles

$N_{aer} = 300/cc$ (two-mode lognormal) $N_{INP} = 150/L$ (lognormal, D_g = 0.74 μm, σ_g = 2.55)

spin-up = freezing off; subsequently frozen particles act as tracers

particle-based μ-physics + prescribed-flow test

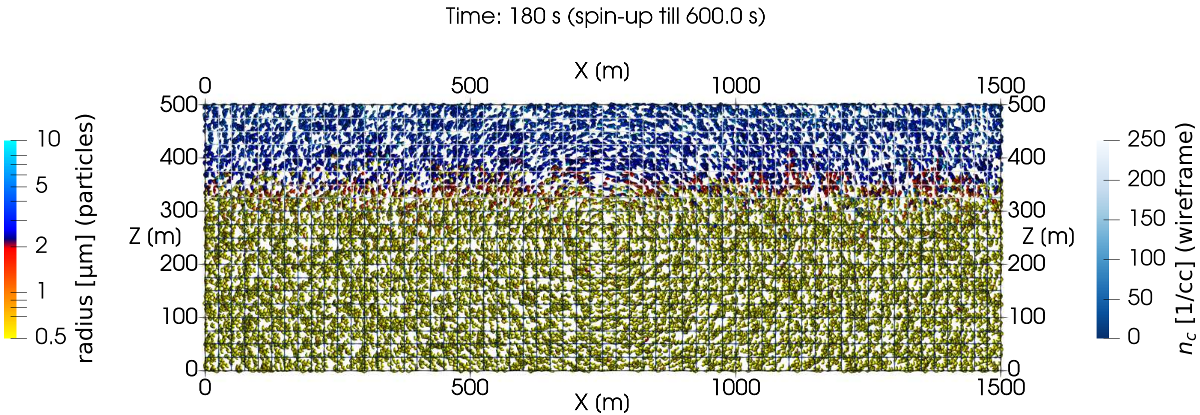

16+16 super-particles/cell for INP-rich + INP-free particles

$N_{aer} = 300/cc$ (two-mode lognormal) $N_{INP} = 150/L$ (lognormal, $D_g = 0.74$ μm, $\sigma_g = 2.55$)

spin-up = freezing off; subsequently frozen particles act as tracers

particle-based μ-physics + prescribed-flow test

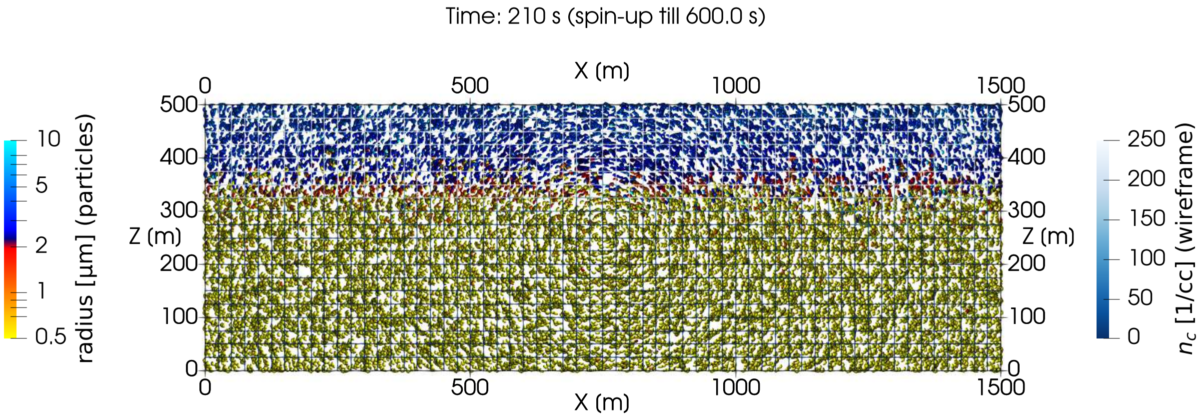

16+16 super-particles/cell for INP-rich + INP-free particles

$N_{aer} = 300/cc$ (two-mode lognormal) $N_{INP} = 150/L$ (lognormal, $D_g = 0.74$ μm, $\sigma_g = 2.55$)

spin-up = freezing off; subsequently frozen particles act as tracers

particle-based μ-physics + prescribed-flow test

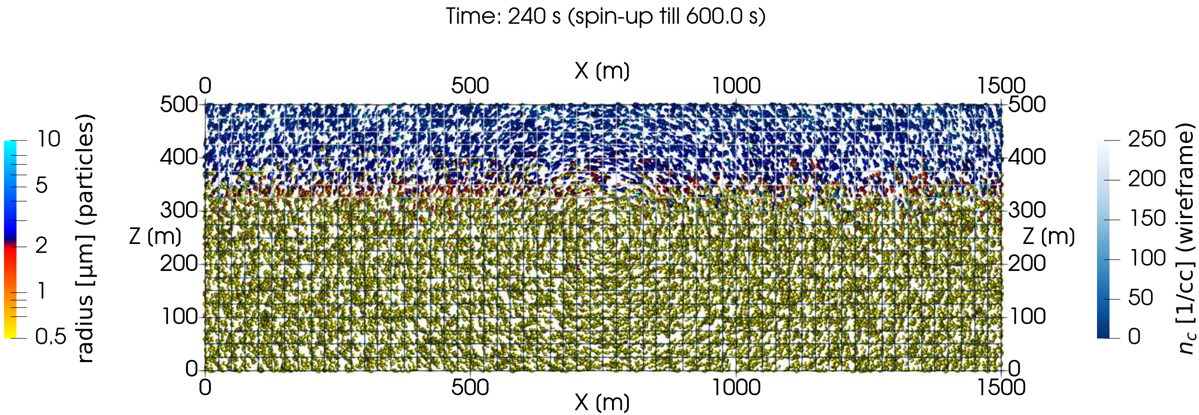

16+16 super-particles/cell for INP-rich + INP-free particles

$N_{aer} = 300/cc$ (two-mode lognormal) $N_{INP} = 150/L$ (lognormal, $D_g = 0.74$ μm, $\sigma_g = 2.55$)

spin-up = freezing off; subsequently frozen particles act as tracers

particle-based μ-physics + prescribed-flow test

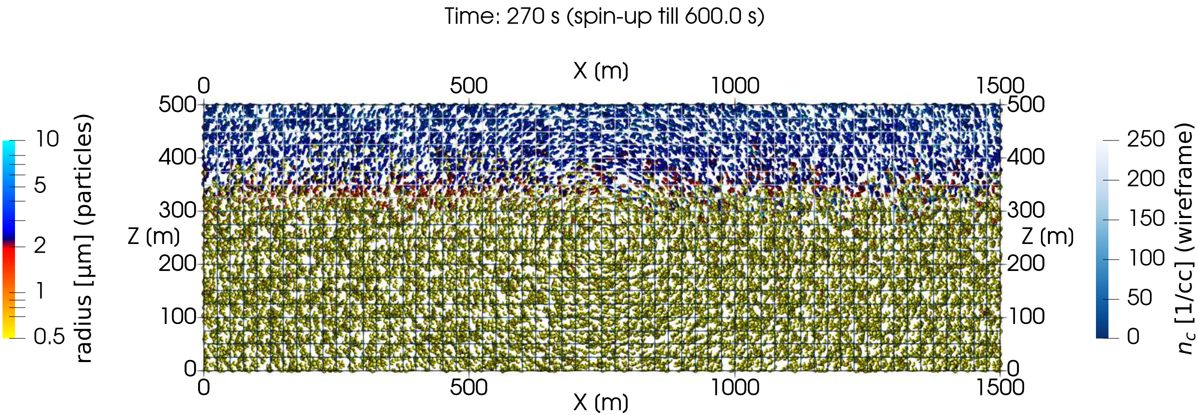

16+16 super-particles/cell for INP-rich + INP-free particles

$N_{aer} = 300/cc$ (two-mode lognormal) $N_{INP} = 150/L$ (lognormal, $D_g = 0.74$ μm, $\sigma_g = 2.55$)

spin-up = freezing off; subsequently frozen particles act as tracers

particle-based μ-physics + prescribed-flow test

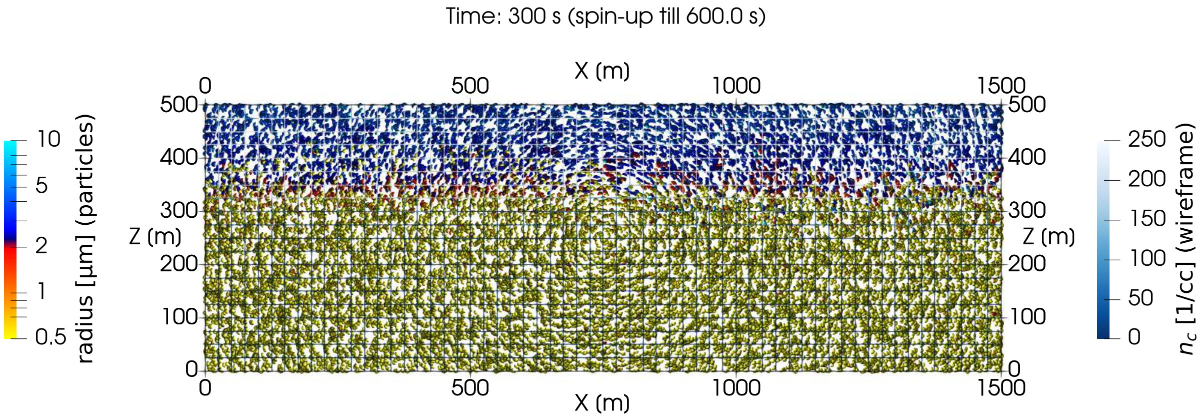

16+16 super-particles/cell for INP-rich + INP-free particles

$N_{aer} = 300/cc$ (two-mode lognormal) $N_{INP} = 150/L$ (lognormal, $D_g = 0.74$ μm, $\sigma_g = 2.55$)

spin-up = freezing off; subsequently frozen particles act as tracers

particle-based μ-physics + prescribed-flow test

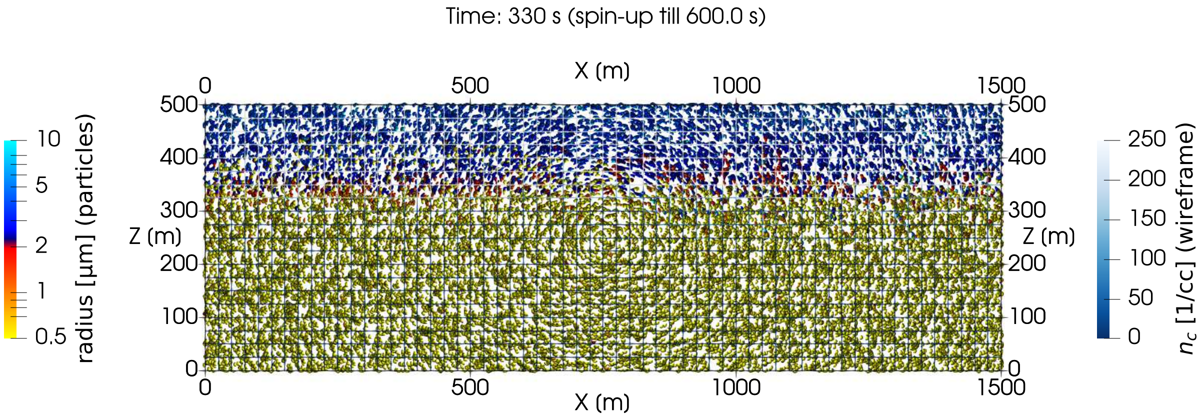

16+16 super-particles/cell for INP-rich + INP-free particles

$N_{\text{aer}} = 300/cc$ (two-mode lognormal) $N_{\text{INP}} = 150/L$ (lognormal, $D_g = 0.74$ μm, $\sigma_g = 2.55$)

spin-up = freezing off; subsequently frozen particles act as tracers

particle-based μ-physics + prescribed-flow test

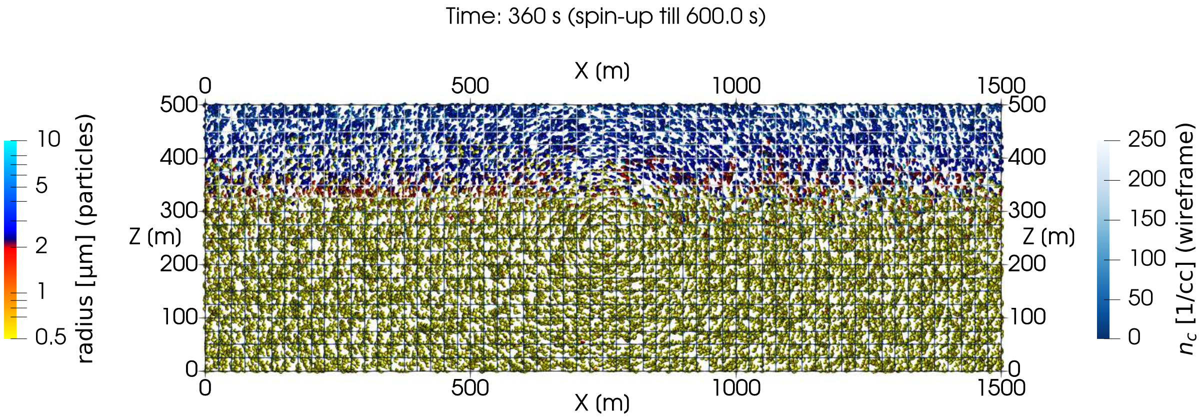

16+16 super-particles/cell for INP-rich + INP-free particles
$N_{aer} = 300/cc$ (two-mode lognormal) $N_{INP} = 150/L$ (lognormal, $D_g = 0.74$ μm, $\sigma_g = 2.55$)
spin-up = freezing off; subsequently frozen particles act as tracers

particle-based μ-physics + prescribed-flow test

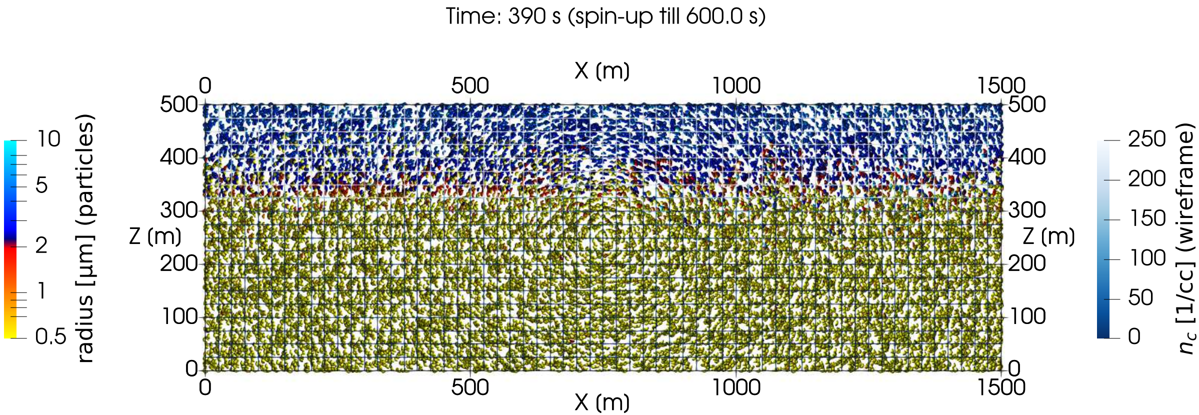

16+16 super-particles/cell for INP-rich + INP-free particles

$N_{aer} = 300/cc$ (two-mode lognormal) $N_{INP} = 150/L$ (lognormal, $D_g = 0.74$ μm, $\sigma_g = 2.55$)

spin-up = freezing off; subsequently frozen particles act as tracers

particle-based μ-physics + prescribed-flow test

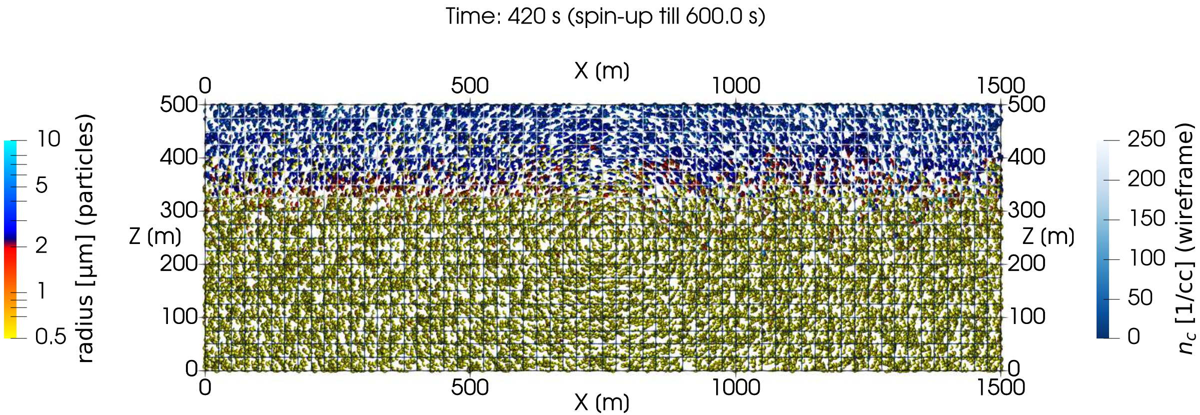

16+16 super-particles/cell for INP-rich + INP-free particles

$N_{aer} = 300/cc$ (two-mode lognormal) $N_{INP} = 150/L$ (lognormal, $D_g = 0.74$ μm, $\sigma_g = 2.55$)

spin-up = freezing off; subsequently frozen particles act as tracers

particle-based μ-physics + prescribed-flow test

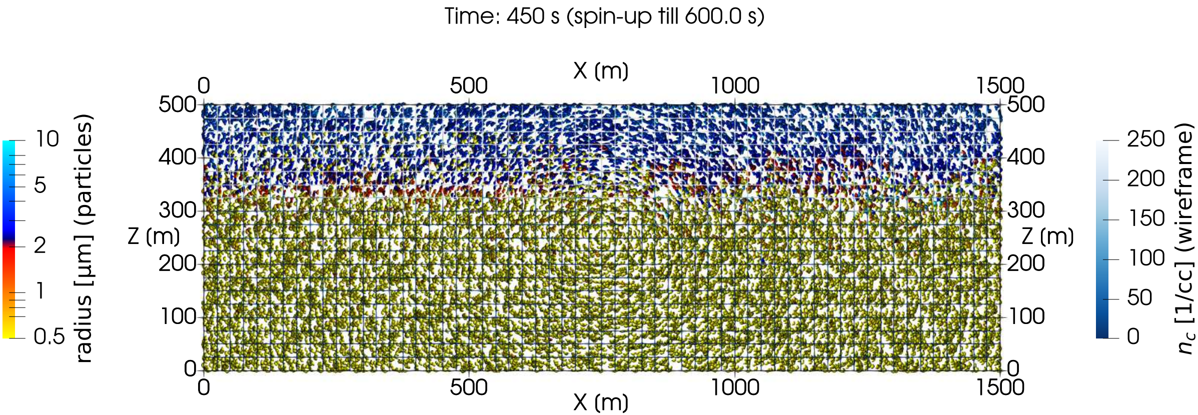

16+16 super-particles/cell for INP-rich + INP-free particles

$N_{aer} = 300/cc$ (two-mode lognormal) $N_{INP} = 150/L$ (lognormal, $D_g = 0.74$ μm, $\sigma_g = 2.55$)

spin-up = freezing off; subsequently frozen particles act as tracers

particle-based μ-physics + prescribed-flow test

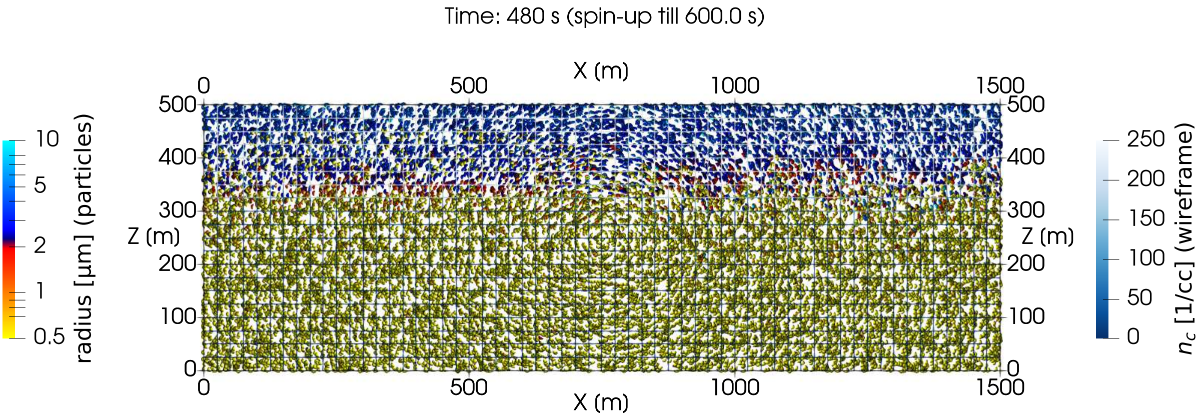

16+16 super-particles/cell for INP-rich + INP-free particles

$N_{\text{aer}} = 300/cc$ (two-mode lognormal) $N_{\text{INP}} = 150/L$ (lognormal, $D_g = 0.74$ μm, $\sigma_g = 2.55$)

spin-up = freezing off; subsequently frozen particles act as tracers

particle-based μ-physics + prescribed-flow test

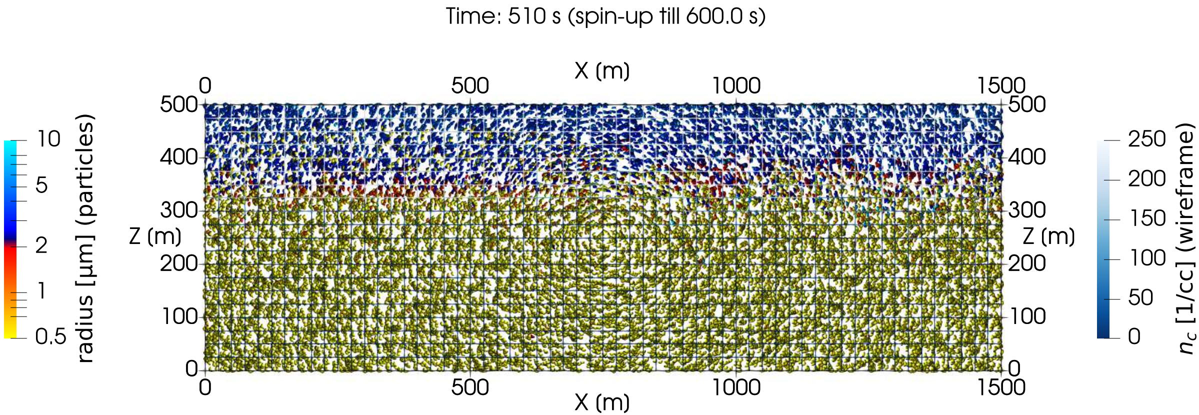

16+16 super-particles/cell for INP-rich + INP-free particles

$N_{\text{aer}} = 300/cc$ (two-mode lognormal) $N_{\text{INP}} = 150/L$ (lognormal, $D_g = 0.74$ μm, $\sigma_g = 2.55$)

spin-up = freezing off; subsequently frozen particles act as tracers

particle-based µ-physics + prescribed-flow test

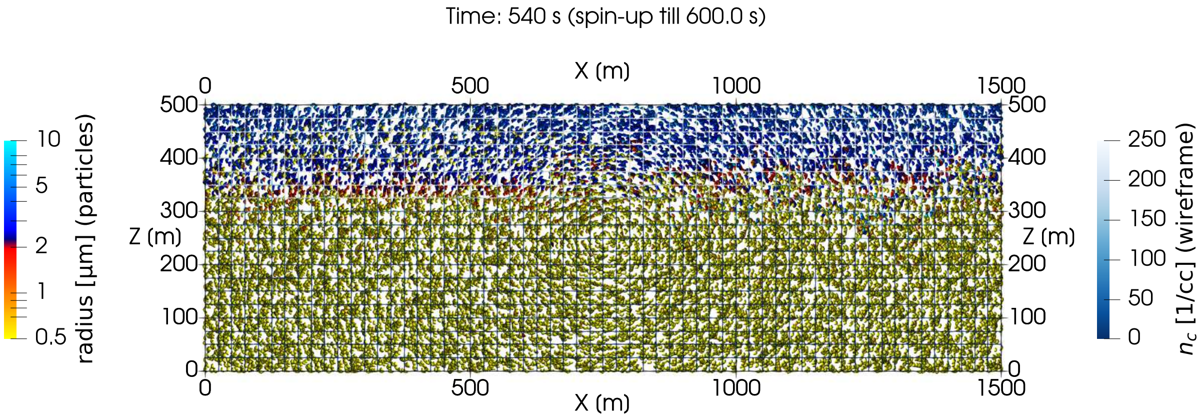

16+16 super-particles/cell for INP-rich + INP-free particles

$N_{aer} = 300/cc$ (two-mode lognormal) $N_{INP} = 150/L$ (lognormal, $D_g = 0.74$ µm, $\sigma_g = 2.55$)

spin-up = freezing off; subsequently frozen particles act as tracers

particle-based μ-physics + prescribed-flow test

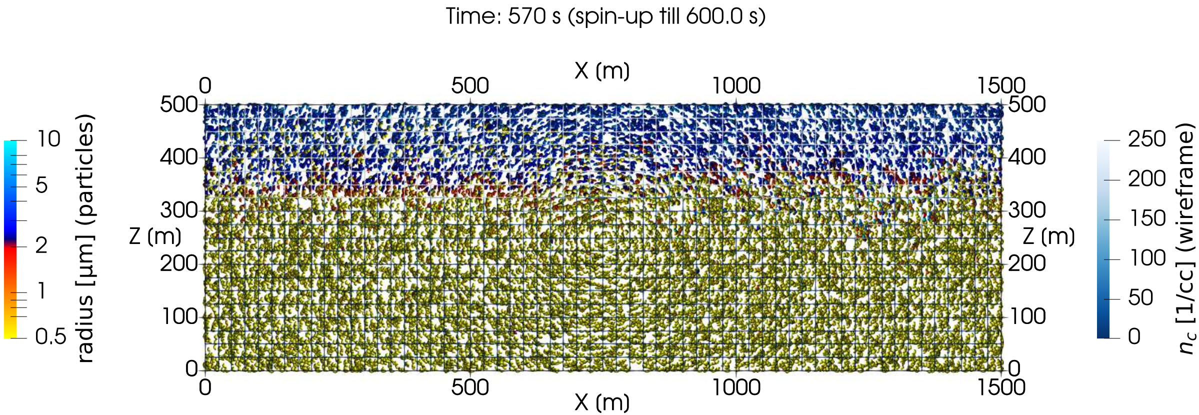

16+16 super-particles/cell for INP-rich + INP-free particles

$N_{aer} = 300/cc$ (two-mode lognormal) $N_{INP} = 150/L$ (lognormal, $D_g = 0.74$ μm, $\sigma_g = 2.55$)

spin-up = freezing off; subsequently frozen particles act as tracers

particle-based µ-physics + prescribed-flow test

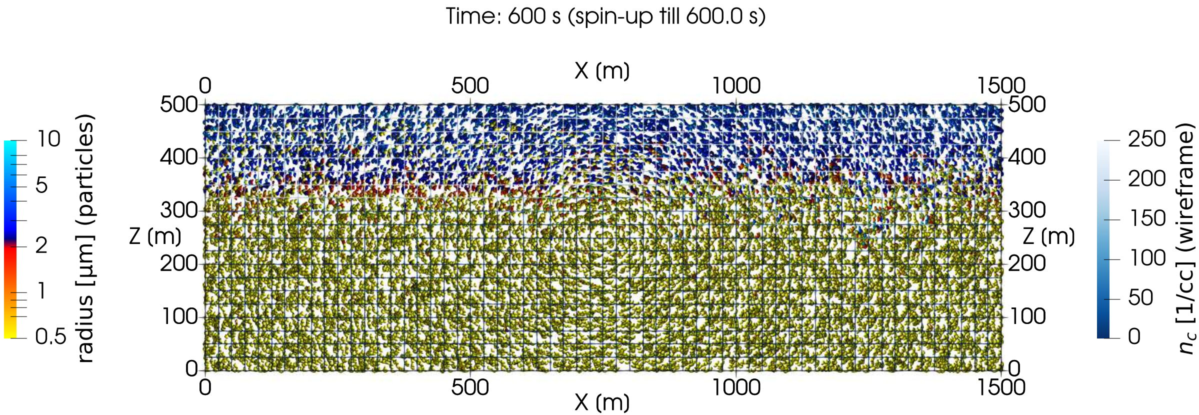

16+16 super-particles/cell for INP-rich + INP-free particles

$N_{aer} = 300/cc$ (two-mode lognormal) $N_{INP} = 150/L$ (lognormal, $D_g = 0.74$ µm, $\sigma_g = 2.55$)

spin-up = freezing off; subsequently frozen particles act as tracers

particle-based µ-physics + prescribed-flow test

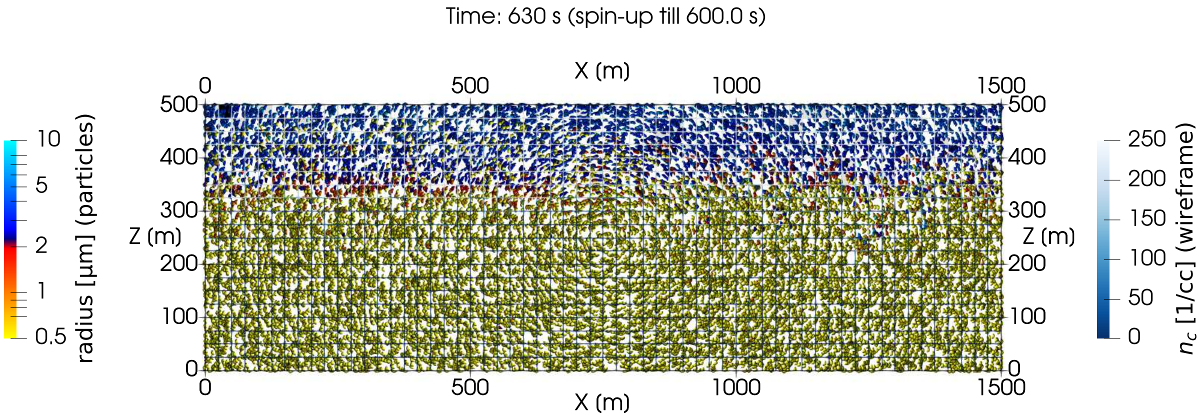

16+16 super-particles/cell for INP-rich + INP-free particles

$N_{aer} = 300/cc$ (two-mode lognormal) $N_{INP} = 150/L$ (lognormal, $D_g = 0.74$ µm, $\sigma_g = 2.55$)

spin-up = freezing off; subsequently frozen particles act as tracers

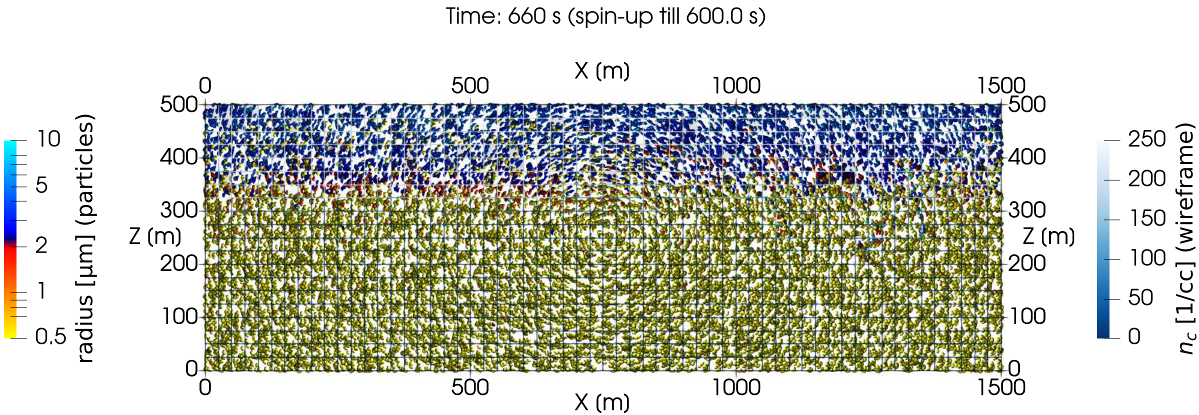

16+16 super-particles/cell for INP-rich + INP-free particles

$N_{aer} = 300/cc$ (two-mode lognormal) $N_{INP} = 150/L$ (lognormal, $D_g = 0.74$ μm, $\sigma_g = 2.55$)

spin-up = freezing off; subsequently frozen particles act as tracers

particle-based μ-physics + prescribed-flow test

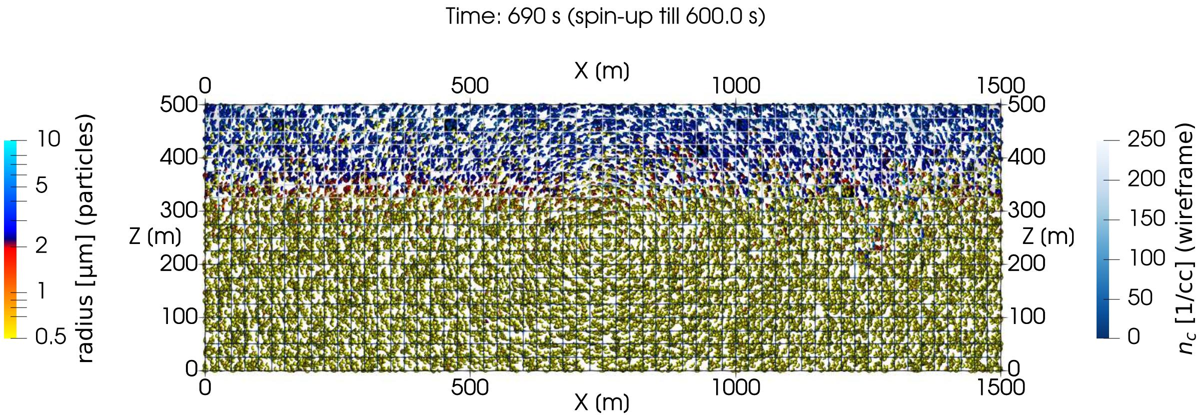

16+16 super-particles/cell for INP-rich + INP-free particles

$N_{\text{aer}} = 300/cc$ (two-mode lognormal) $N_{\text{INP}} = 150/L$ (lognormal, $D_g = 0.74$ μm, $\sigma_g = 2.55$)

spin-up = freezing off; subsequently frozen particles act as tracers

particle-based μ-physics + prescribed-flow test

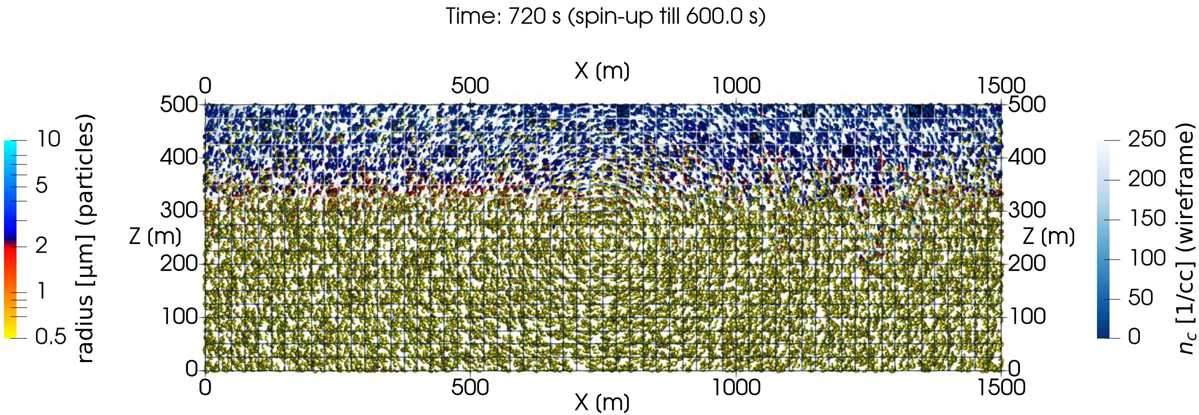

16+16 super-particles/cell for INP-rich + INP-free particles

$N_{aer} = 300/cc$ (two-mode lognormal) $N_{INP} = 150/L$ (lognormal, $D_g = 0.74$ μm, $\sigma_g = 2.55$)

spin-up = freezing off; subsequently frozen particles act as tracers

particle-based μ-physics + prescribed-flow test

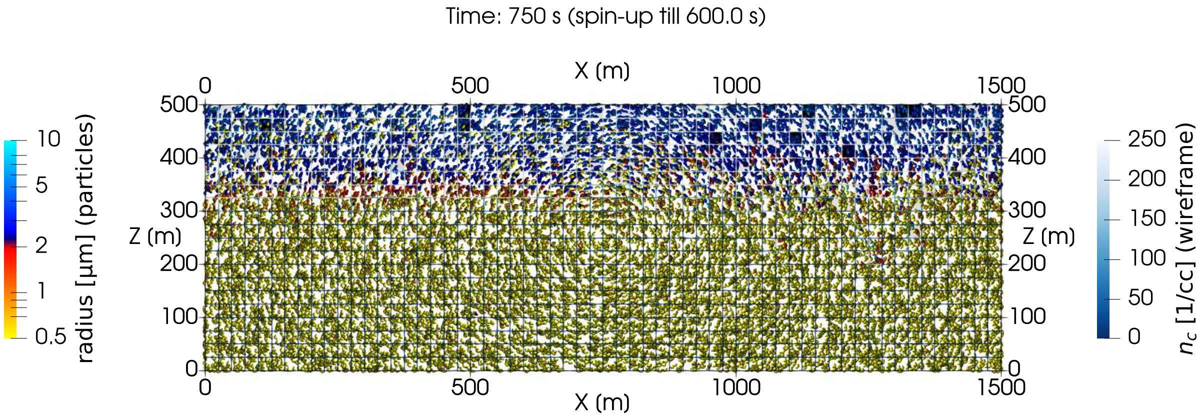

16+16 super-particles/cell for INP-rich + INP-free particles

$N_{\text{aer}} = 300/cc$ (two-mode lognormal) $N_{\text{INP}} = 150/L$ (lognormal, $D_g = 0.74$ μm, $\sigma_g = 2.55$)

spin-up = freezing off; subsequently frozen particles act as tracers

particle-based μ-physics + prescribed-flow test

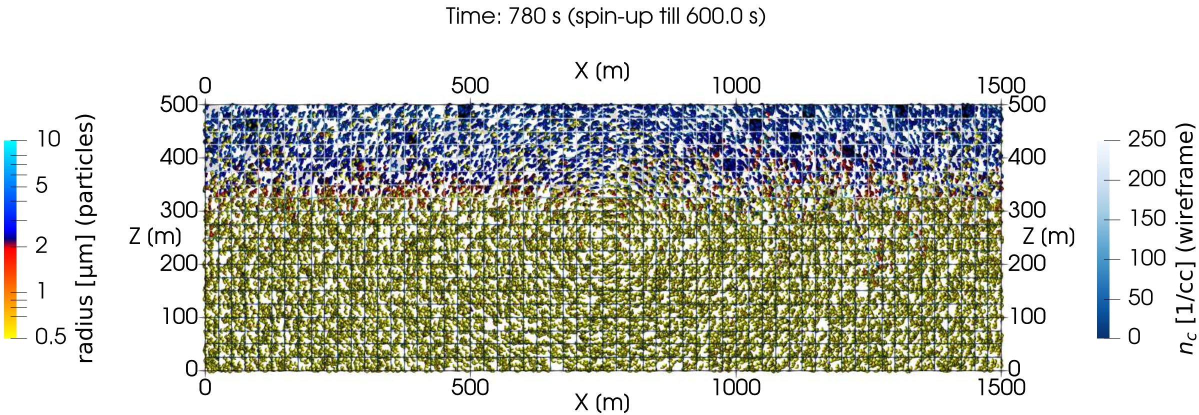

16+16 super-particles/cell for INP-rich + INP-free particles

$N_{\text{aer}} = 300/cc$ (two-mode lognormal) $N_{\text{INP}} = 150/L$ (lognormal, $D_g = 0.74$ μm, $\sigma_g = 2.55$)

spin-up = freezing off; subsequently frozen particles act as tracers

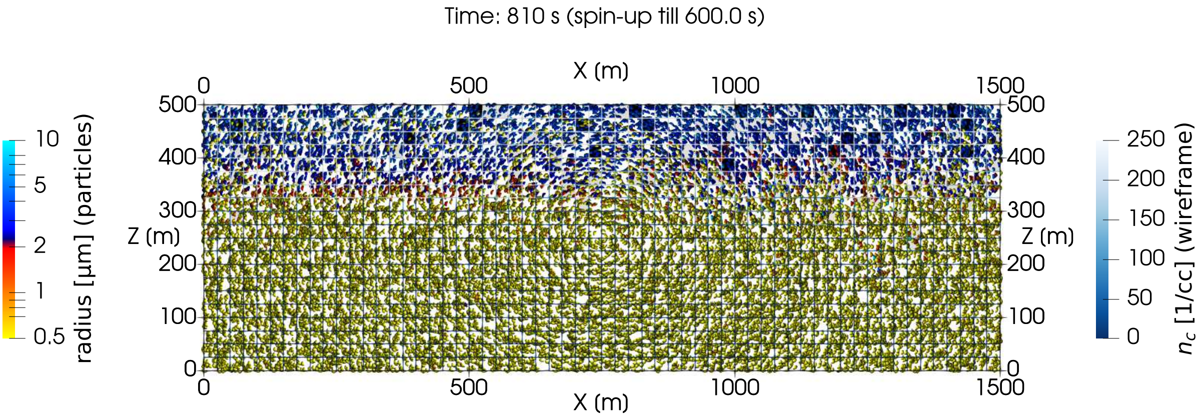

16+16 super-particles/cell for INP-rich + INP-free particles

$N_{aer} = 300/cc$ (two-mode lognormal) $N_{INP} = 150/L$ (lognormal, $D_g = 0.74$ μm, $\sigma_g = 2.55$)

spin-up = freezing off; subsequently frozen particles act as tracers

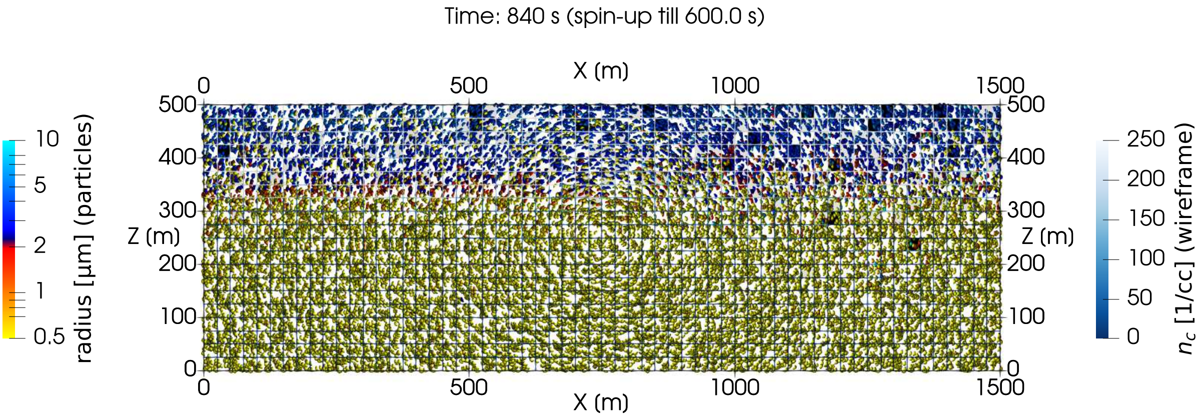

16+16 super-particles/cell for INP-rich + INP-free particles

$N_{\text{aer}} = 300/cc$ (two-mode lognormal) $N_{\text{INP}} = 150/L$ (lognormal, $D_g = 0.74$ μm, $\sigma_g = 2.55$)

spin-up = freezing off; subsequently frozen particles act as tracers

particle-based μ-physics + prescribed-flow test

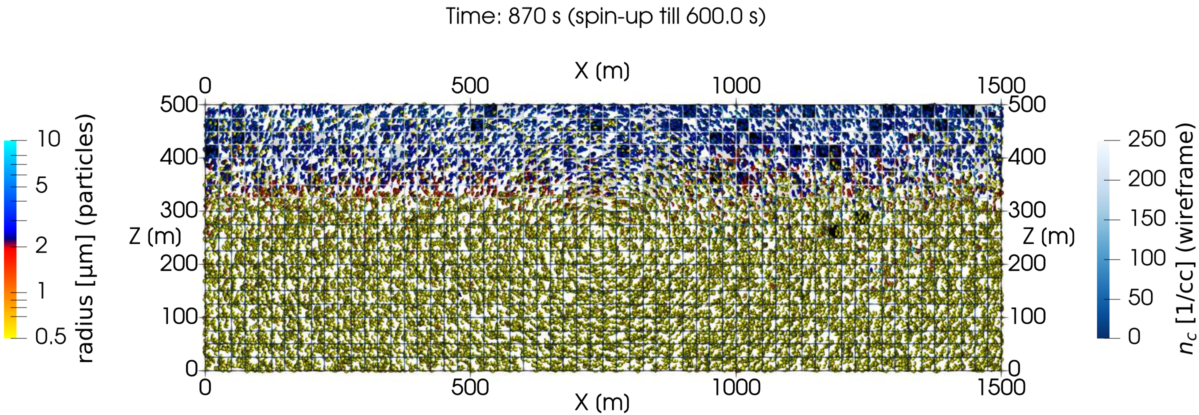

16+16 super-particles/cell for INP-rich + INP-free particles

$N_{aer} = 300/cc$ (two-mode lognormal) $N_{INP} = 150/L$ (lognormal, $D_g = 0.74$ μm, $\sigma_g = 2.55$)

spin-up = freezing off; subsequently frozen particles act as tracers

particle-based μ-physics + prescribed-flow test

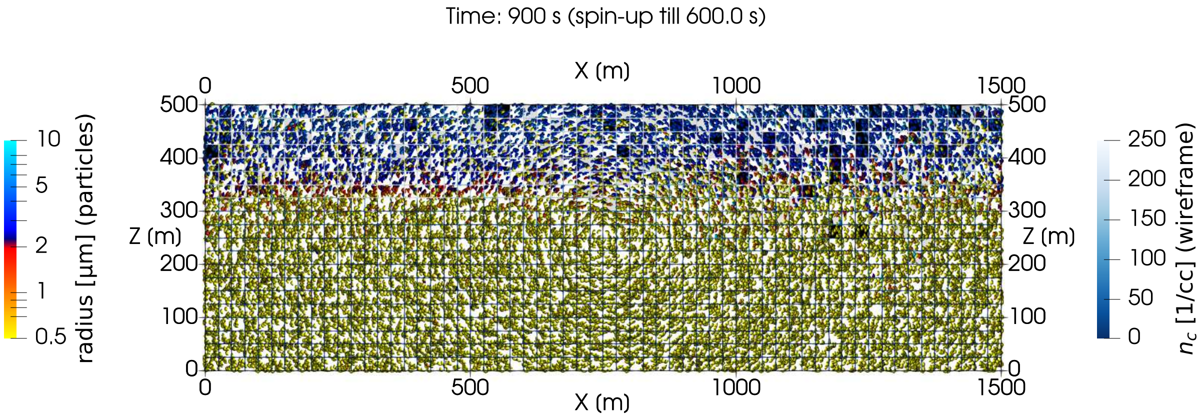

16+16 super-particles/cell for INP-rich + INP-free particles

$N_{\text{aer}} = 300/cc$ (two-mode lognormal) $N_{\text{INP}} = 150/L$ (lognormal, $D_g = 0.74$ μm, $\sigma_g = 2.55$)

spin-up = freezing off; subsequently frozen particles act as tracers

particle-based μ-physics + prescribed-flow test

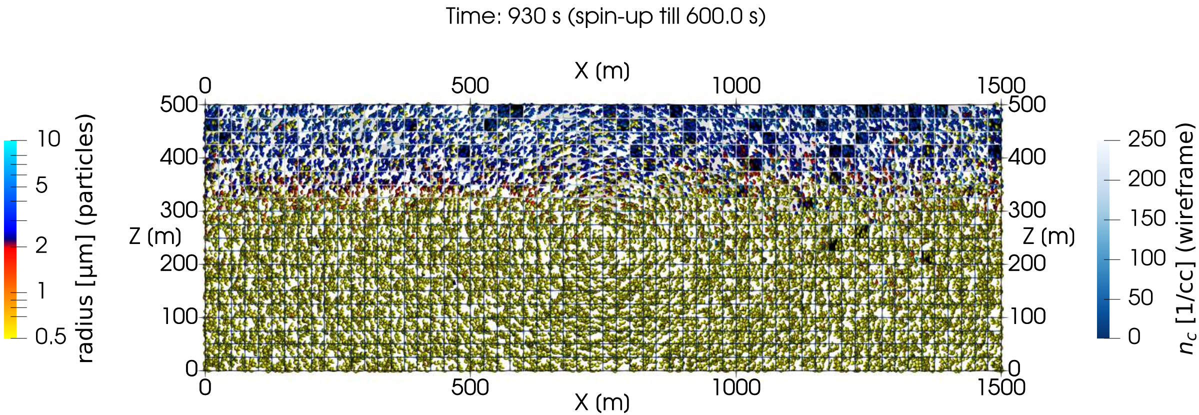

16+16 super-particles/cell for INP-rich + INP-free particles

$N_{\text{aer}} = 300/cc$ (two-mode lognormal) $N_{\text{INP}} = 150/L$ (lognormal, $D_g = 0.74$ μm, $\sigma_g = 2.55$)

spin-up = freezing off; subsequently frozen particles act as tracers

particle-based μ-physics + prescribed-flow test

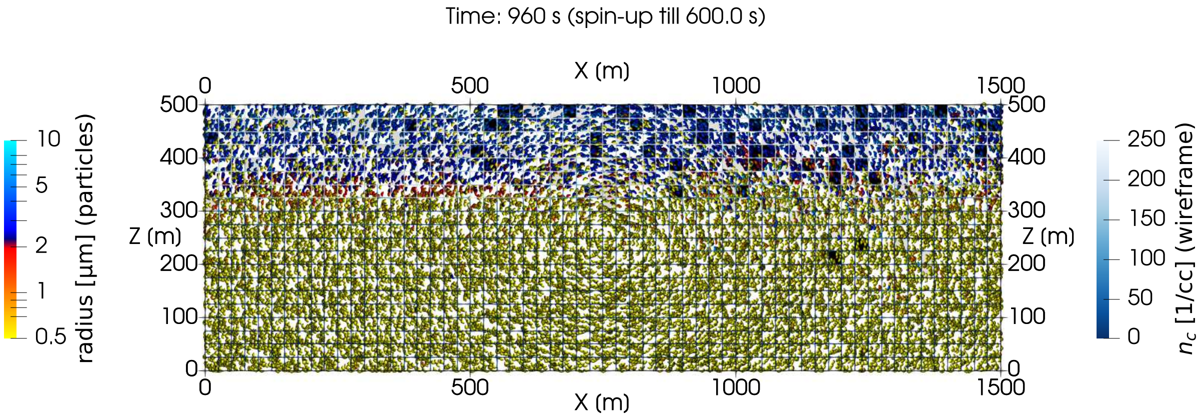

16+16 super-particles/cell for INP-rich + INP-free particles

$N_{\text{aer}} = 300/cc$ (two-mode lognormal) $N_{\text{INP}} = 150/L$ (lognormal, $D_g = 0.74$ μm, $\sigma_g = 2.55$)

spin-up = freezing off; subsequently frozen particles act as tracers

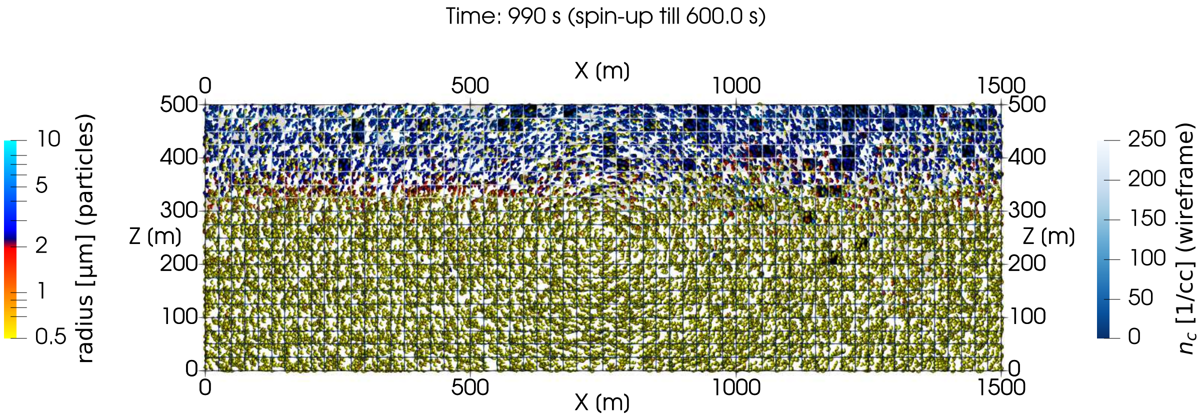

16+16 super-particles/cell for INP-rich + INP-free particles

$N_{\text{aer}} = 300/cc$ (two-mode lognormal) $N_{\text{INP}} = 150/L$ (lognormal, $D_g = 0.74$ μm, $\sigma_g = 2.55$)

spin-up = freezing off; subsequently frozen particles act as tracers

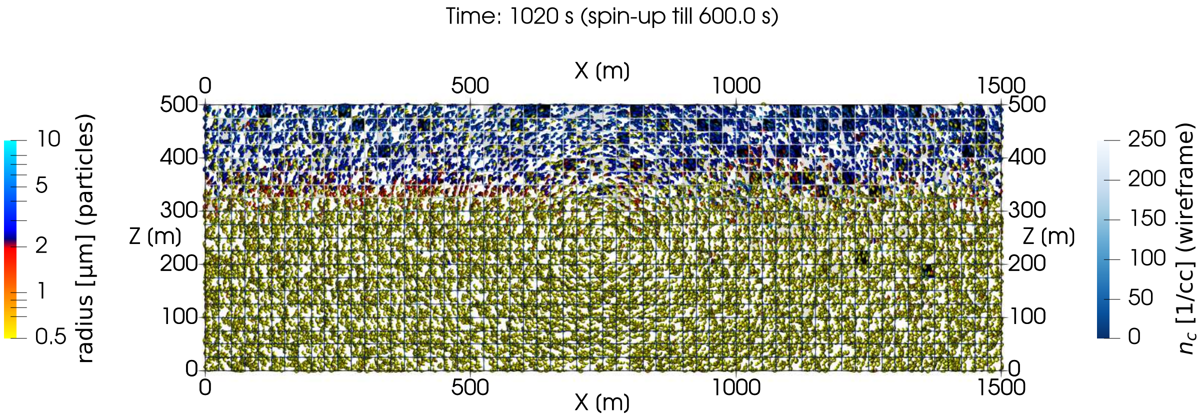

16+16 super-particles/cell for INP-rich + INP-free particles

$N_{aer} = 300/cc$ (two-mode lognormal) $N_{INP} = 150/L$ (lognormal, $D_g = 0.74$ μm, $\sigma_g = 2.55$)

spin-up = freezing off; subsequently frozen particles act as tracers

particle-based μ-physics + prescribed-flow test

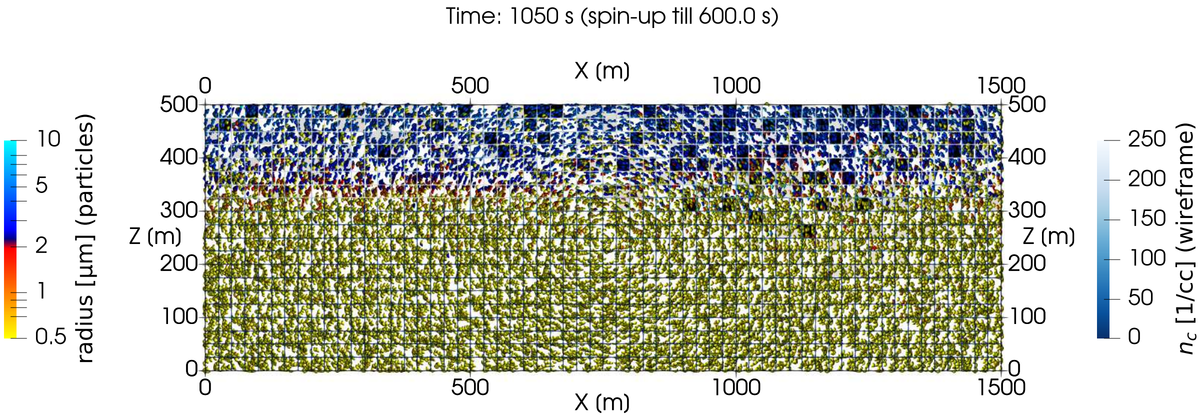

16+16 super-particles/cell for INP-rich + INP-free particles

$N_{\text{aer}} = 300/cc$ (two-mode lognormal) $N_{\text{INP}} = 150/L$ (lognormal, $D_g = 0.74$ μm, $\sigma_g = 2.55$)

spin-up = freezing off; subsequently frozen particles act as tracers

particle-based μ-physics + prescribed-flow test

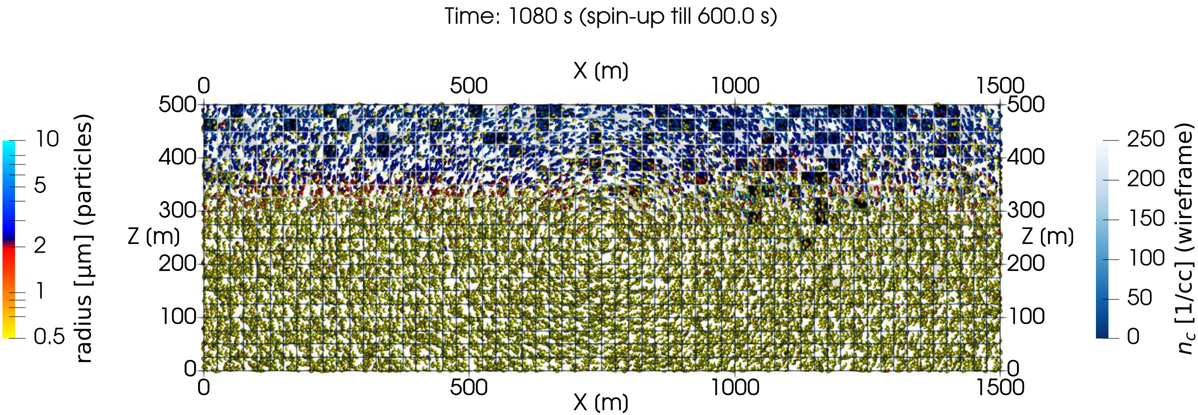

16+16 super-particles/cell for INP-rich + INP-free particles

$N_{aer} = 300/cc$ (two-mode lognormal) $N_{INP} = 150/L$ (lognormal, $D_g = 0.74$ μm, $\sigma_g = 2.55$)

spin-up = freezing off; subsequently frozen particles act as tracers

particle-based μ-physics + prescribed-flow test

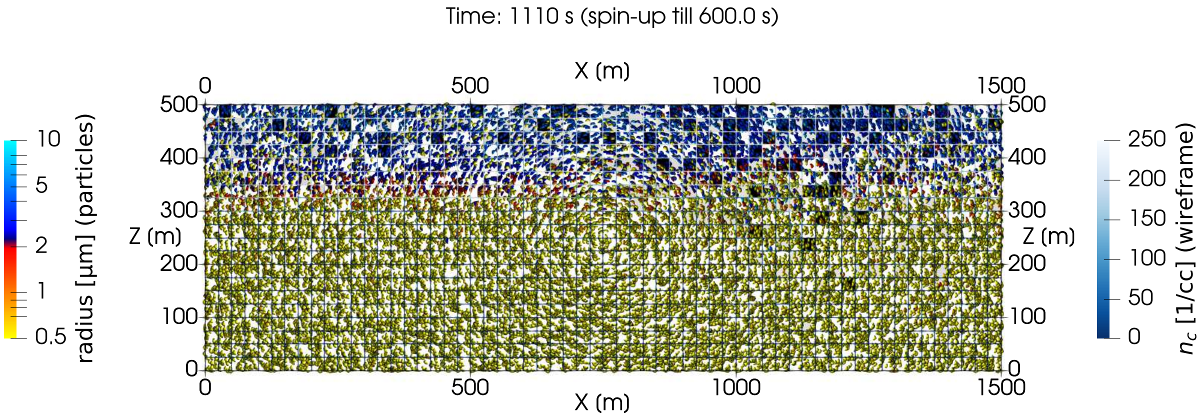

16+16 super-particles/cell for INP-rich + INP-free particles

$N_{\text{aer}} = 300/cc$ (two-mode lognormal) $N_{\text{INP}} = 150/L$ (lognormal, $D_g = 0.74$ μm, $\sigma_g = 2.55$)

spin-up = freezing off; subsequently frozen particles act as tracers

particle-based µ-physics + prescribed-flow test

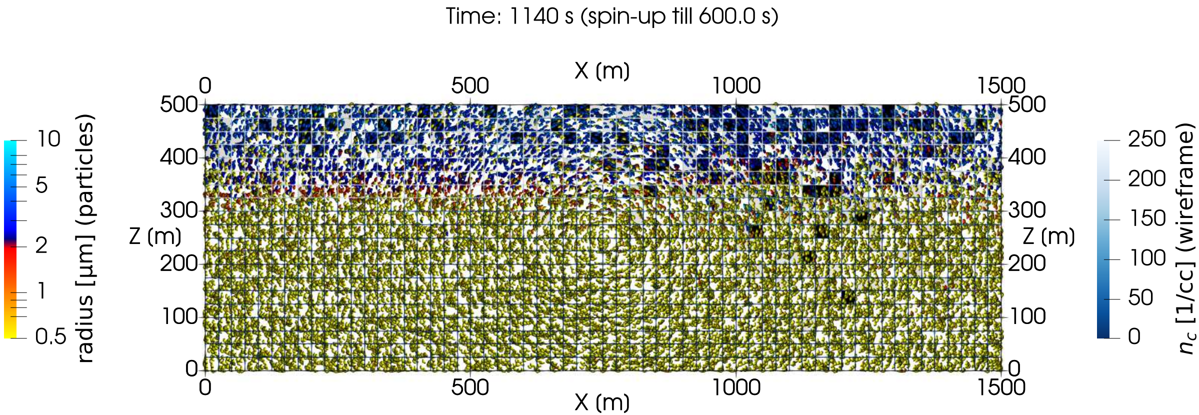

16+16 super-particles/cell for INP-rich + INP-free particles

$N_{aer} = 300/cc$ (two-mode lognormal) $N_{INP} = 150/L$ (lognormal, $D_g = 0.74$ µm, $\sigma_g = 2.55$)

spin-up = freezing off; subsequently frozen particles act as tracers

particle-based μ-physics + prescribed-flow test

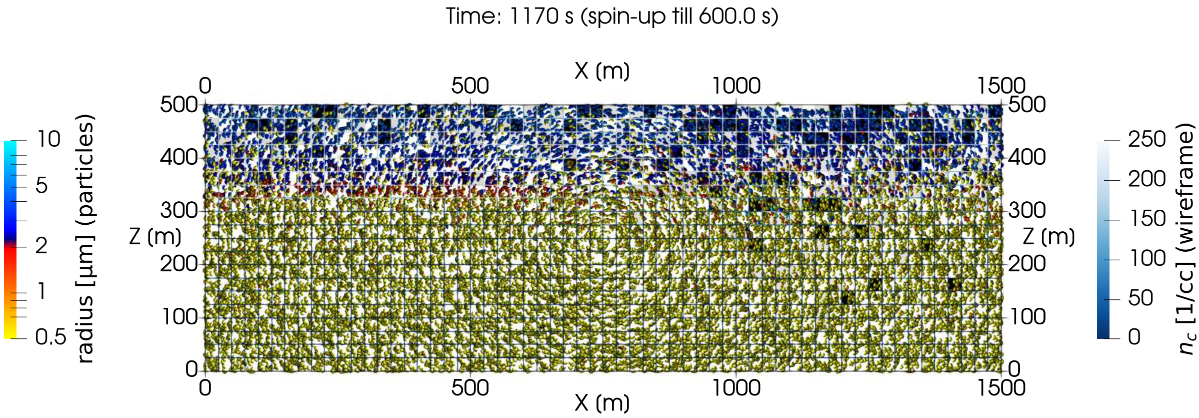

16+16 super-particles/cell for INP-rich + INP-free particles

$N_{\text{aer}} = 300/cc$ (two-mode lognormal) $N_{\text{INP}} = 150/L$ (lognormal, $D_g = 0.74$ μm, $\sigma_g = 2.55$)

spin-up = freezing off; subsequently frozen particles act as tracers

particle-based μ-physics + prescribed-flow test

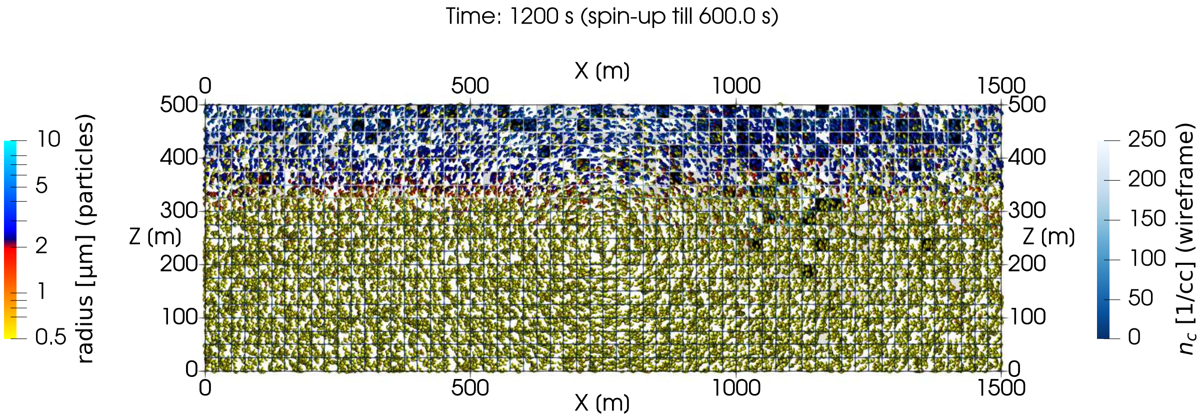

16+16 super-particles/cell for INP-rich + INP-free particles

$N_{aer} = 300/cc$ (two-mode lognormal) $N_{INP} = 150/L$ (lognormal, $D_g = 0.74$ μm, $\sigma_g = 2.55$)

spin-up = freezing off; subsequently frozen particles act as tracers

testing three flow regimes and two immersion freezing representations

$w_{max} \approx 1/3$ m/s

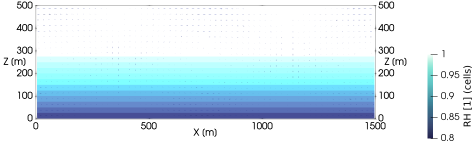

$w_{max} \approx 1$ m/s

$w_{max} \approx 3$ m/s

testing three flow regimes and two immersion freezing representations

$w_{max} \approx 1/3$ m/s

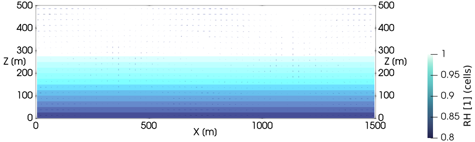

$w_{max} \approx 1$ m/s

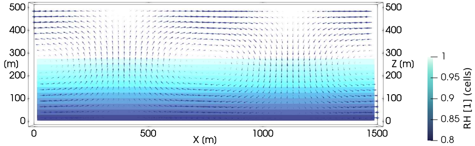

$w_{max} \approx 3$ m/s

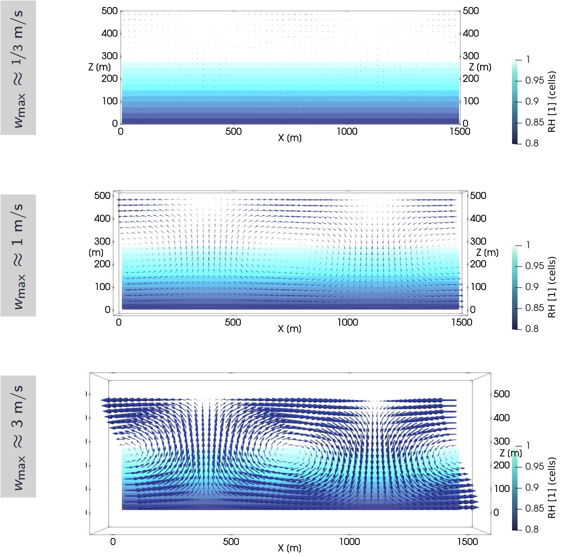
wmax ≈ 1/3 m/s
wmax ≈ 1 m/s
wmax ≈ 3 m/s
Z (m)
X (m)
RH [1] (cells)
0.8
0.85
0.9
0.95
1

testing three flow regimes and two immersion freezing representations

$w_{max} \approx 1/3$ m/s

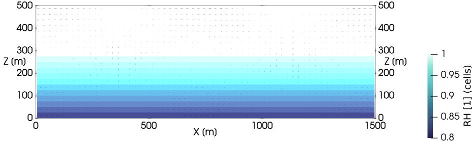

$w_{max} \approx 1$ m/s

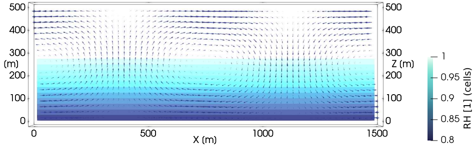

$w_{max} \approx 3$ m/s

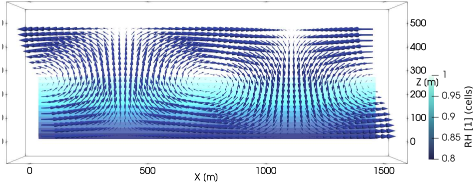

singular (INAS)

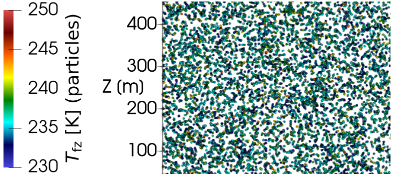

time-dependent (J_{het})

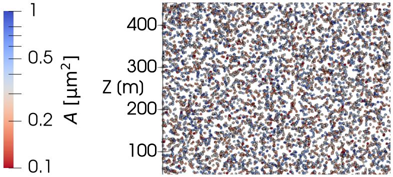

testing three flow regimes and two immersion freezing representations

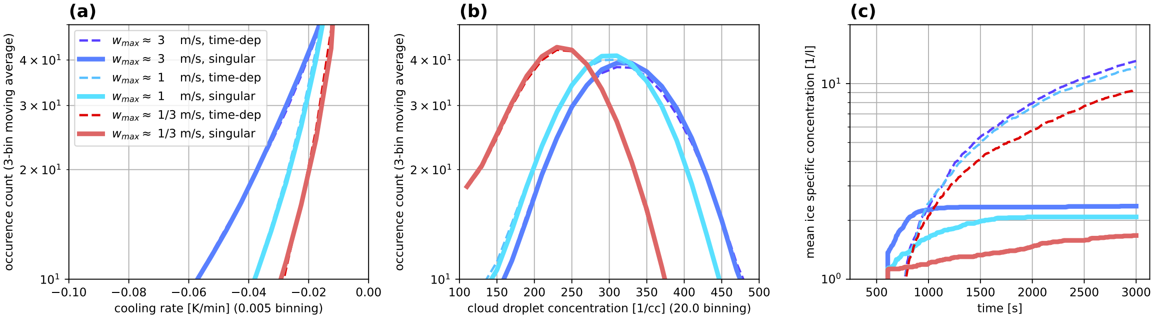

- range of cooling rates in simple flow (far from $c \sim 1$ K/min for AIDA as in Niemand et al. 2012)

testing three flow regimes and two immersion freezing representations

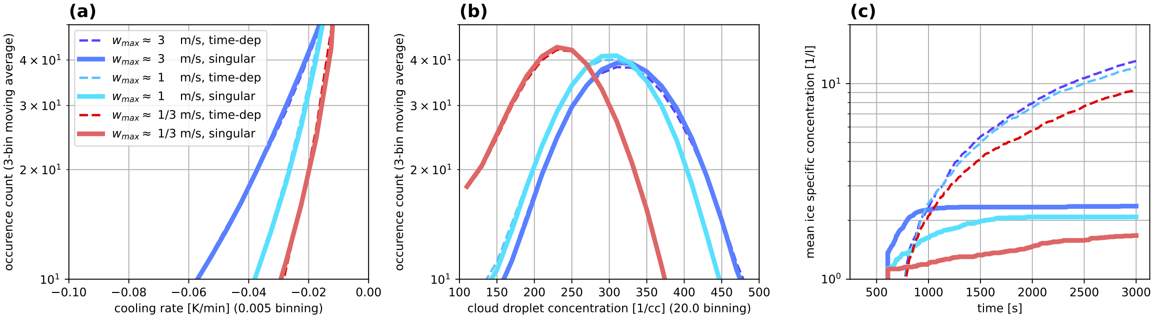

- range of cooling rates in simple flow (far from $c \sim 1$ K/min for AIDA as in Niemand et al. 2012)
- singular vs. time-dependent markedly different (consistent with box model for $c \ll 1K/min$)

testing three flow regimes and two immersion freezing representations

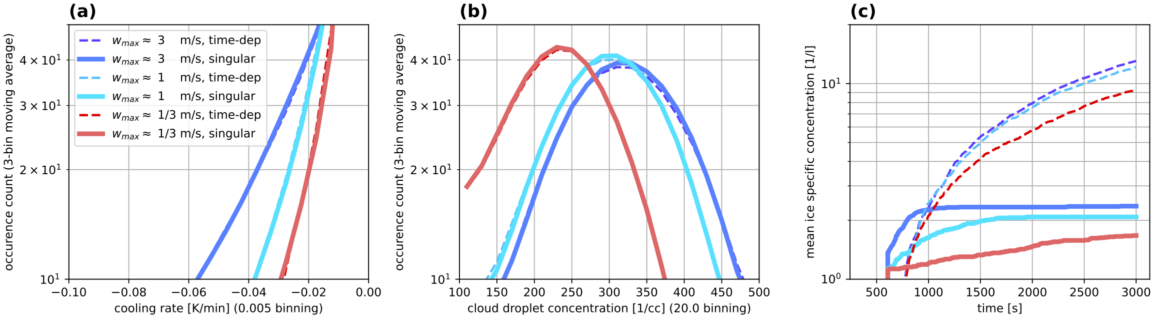

- range of cooling rates in simple flow (far from $c \sim 1$ K/min for AIDA as in Niemand et al. 2012)
- singular vs. time-dependent markedly different (consistent with box model for $c \ll 1K/min$)
- CPU time trade off: time dependent ca. 3-4 times costlier

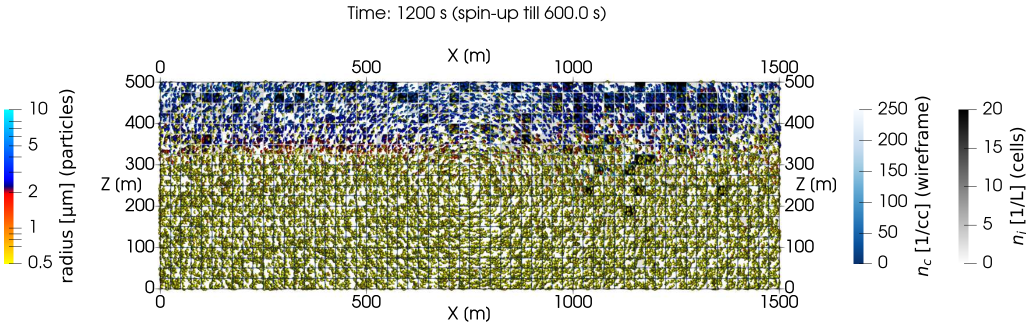

key messages:

– emergence of comprehensive mixed-phase particle-based aerosol/cloud µ-physics models

– cooling rate embedded in INAS fits ⇝ limited robustness to different flow regimes

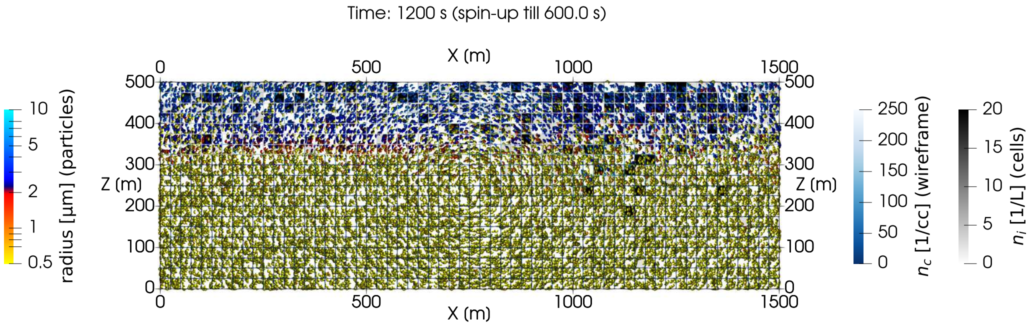

key messages:

– emergence of comprehensive mixed-phase particle-based aerosol/cloud μ-physics models

– cooling rate embedded in INAS fits ⇝ limited robustness to different flow regimes

ASR Atmospheric System Research

DOE ASR grant no.
DE-SC0021034

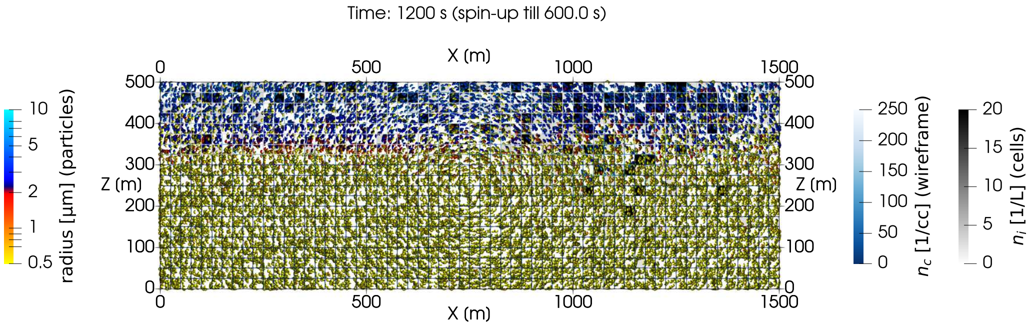

key messages:

– emergence of comprehensive mixed-phase particle-based aerosol/cloud μ-physics models

– cooling rate embedded in INAS fits ⇝ limited robustness to different flow regimes

ASR Atmospheric System Research DOE ASR grant no. DE-SC0021034

project hosted at: ILLINOIS

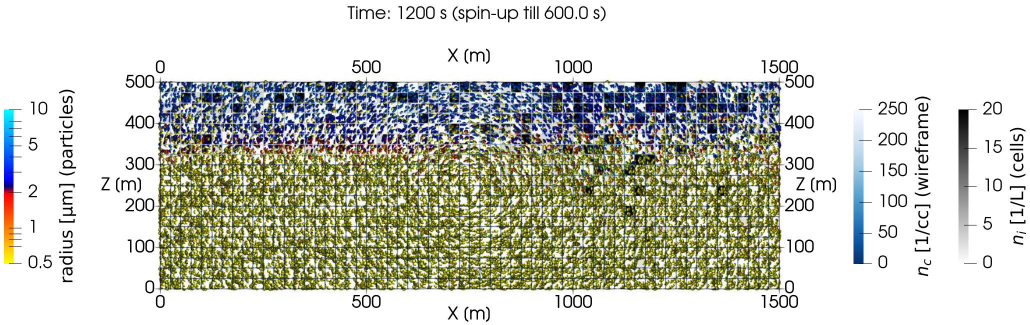

key messages:

– emergence of comprehensive mixed-phase particle-based aerosol/cloud μ-physics models

– cooling rate embedded in INAS fits ⇝ limited robustness to different flow regimes

ASR Atmospheric System Research DOE ASR grant no. DE-SC0021034

project hosted at: ILLINOIS

open python code: /atmos-cloud-sim-uj

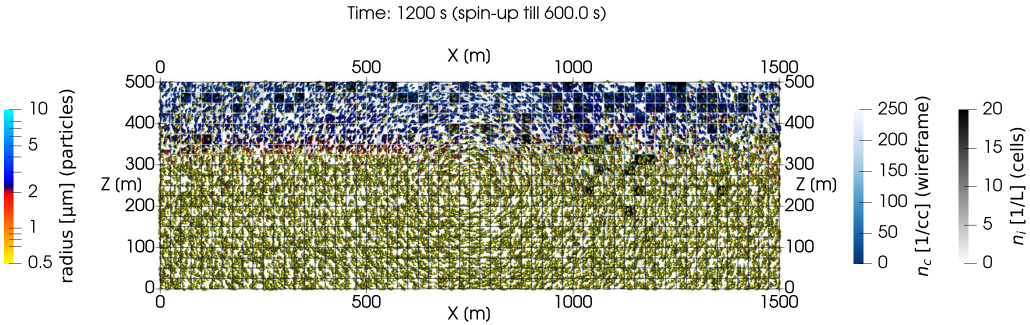

key messages:

– emergence of comprehensive mixed-phase particle-based aerosol/cloud µ-physics models

– cooling rate embedded in INAS fits ⇝ limited robustness to different flow regimes

ASR Atmospheric System Research DOE ASR grant no. DE-SC0021034

project hosted at: ILLINOIS

open python code: /atmos-cloud-sim-uj

Thank you for your attention!